Heterosis of leaf and rhizosphere microbiomes in field-grown maize

Maggie R. Wagner[1,2], Joe H. Roberts[3], Peter Balint-Kurti[3,4], James B. Holland[4,5]

[1] Department of Ecology and Evolutionary Biology, University of Kansas, Lawrence, KS 66045
[2] Kansas Biological Survey, University of Kansas, Lawrence, KS 66045
[3] Department of Entomology and Plant Pathology, North Carolina State University, Raleigh, NC 27695
[4] Plant Science Research Unit, Agricultural Research Service, United States Department of Agriculture, Raleigh, NC 27695
[5] Department of Crop and Soil Sciences, North Carolina State University, Raleigh, NC 27695

Correspondence and requests for materials should be addressed to M.R.W.
Department of Ecology and Evolutionary Biology
University of Kansas
1200 Sunnyside Avenue, Lawrence, KS, 66045, USA
maggie.r.wagner@ku.edu

Word count (Total): 7411
Word count (Introduction): 766
Word count (Methods): 3356
Word count (Results): 1640
Word count (Discussion): 1649

Number of figures: 6 (all in color)
Number of tables: 1
Supporting Information: 7 tables + 10 figures (all in color)
Word count (Acknowledgements): 113

Summary:

- Macroorganisms' genotypes shape their phenotypes, which in turn shape the habitat available to potential microbial symbionts. This influence of host genotype on microbiome composition has been demonstrated in many systems; however, most previous studies have either compared unrelated genotypes or delved into molecular mechanisms. As a result, it is currently unclear whether the heritability of host-associated microbiomes follows similar patterns to the heritability of other complex traits.
- We take a new approach to this question by comparing the microbiomes of diverse maize inbred lines and their F_1 hybrid offspring, which we quantified in both rhizosphere and leaves of field-grown plants using 16S-v4 and ITS1 amplicon sequencing.
- We show that inbred lines and hybrids differ consistently in composition of bacterial and fungal rhizosphere communities, as well as leaf-associated fungal communities. A wide range of microbiome features display heterosis within individual crosses, consistent with patterns for non-microbial maize phenotypes. For leaf microbiomes, these results were supported by the observation that broad-sense heritability in hybrids was substantially higher than narrow-sense heritability.
- Our results support our hypothesis that at least some heterotic host traits affect microbiome composition in maize.

Key words: heterosis; hybridization; maize; microbiome; phyllosphere; rhizosphere

INTRODUCTION

The role of host genotype in shaping microbiome composition and function is a crucial topic for both basic and applied research into plant-associated microbial communities. Understanding patterns and mechanisms of microbiome heritability is a key step toward understanding how plant-microbiome interactions evolved, and unlocking their potential to improve agricultural productivity and sustainability (Bordenstein & Theis, 2015; Busby *et al.*, 2017). Heritable components of microbiome variation may reflect plant-microbe interactions that have been shaped by natural selection acting on plant traits underlying fitness, which might be modified during crop breeding. Plant genotype can also affect the phenotypic response to variation in the local microbial species pool. Thus, genetic variation within and among species may have major implications for harnessing the potential benefits of plant-associated microbiomes, which include improved nutrient acquisition, drought resistance, defense, and reproductive phenology (Friesen *et al.*, 2011; Lau & Lennon, 2012; Wagner *et al.*, 2014; Panke-Buisse *et al.*, 2015, 2017; Santhanam *et al.*, 2015; Busby *et al.*, 2016; Ritpitakphong *et al.*, 2016; Berg & Koskella, 2018; Hubbard *et al.*, 2019).

Although many studies have documented host genetic variation for microbiome composition, most of these have compared genotypes whose relationship to each other is undefined (Bodenhausen *et al.*, 2013; Edwards *et al.*, 2015; Wagner *et al.*, 2016; Wallace *et al.*, 2018a; Walters *et al.*, 2018) or delved into molecular mechanisms using mutants, transgenic manipulation, or QTL-mapping approaches (Bressan *et al.*, 2009; Bodenhausen *et al.*, 2014; Horton *et al.*, 2014; Beckers *et al.*, 2016; Ritpitakphong *et al.*, 2016). As a result, we have limited ability to predict microbiome similarity between two host genotypes that are directly related (*e.g.,* within a known pedigree). Recently, the introgression of quantitative trait loci was shown to alter leaf microbiomes across five generations of a breeding experiment for improved disease resistance in maize (Wagner *et al.*, 2020); however, additional studies of this type are needed before we will be able to anticipate what microbiome changes might follow genetic improvement in crops or evolution in natural populations.

One major outstanding question is whether hybridization between genetically distinct lineages results in hybrids that harbor microbiomes that are intermediate in composition between those of the parent genotypes. This question is important because intermating between diverged populations or species can create novel combinations of alleles that modify adaptively important traits, with major evolutionary implications (Anderson & Stebbins, 1954; Soltis & Soltis, 2009). Hybridization is also the cornerstone of many crop breeding strategies. In

71 many cases, and particularly in maize, traits of hybrids exceed both of their parents rather than
72 being intermediate between their parents. This results in more robust, productive plants—a
73 phenomenon known as heterosis or hybrid vigor.

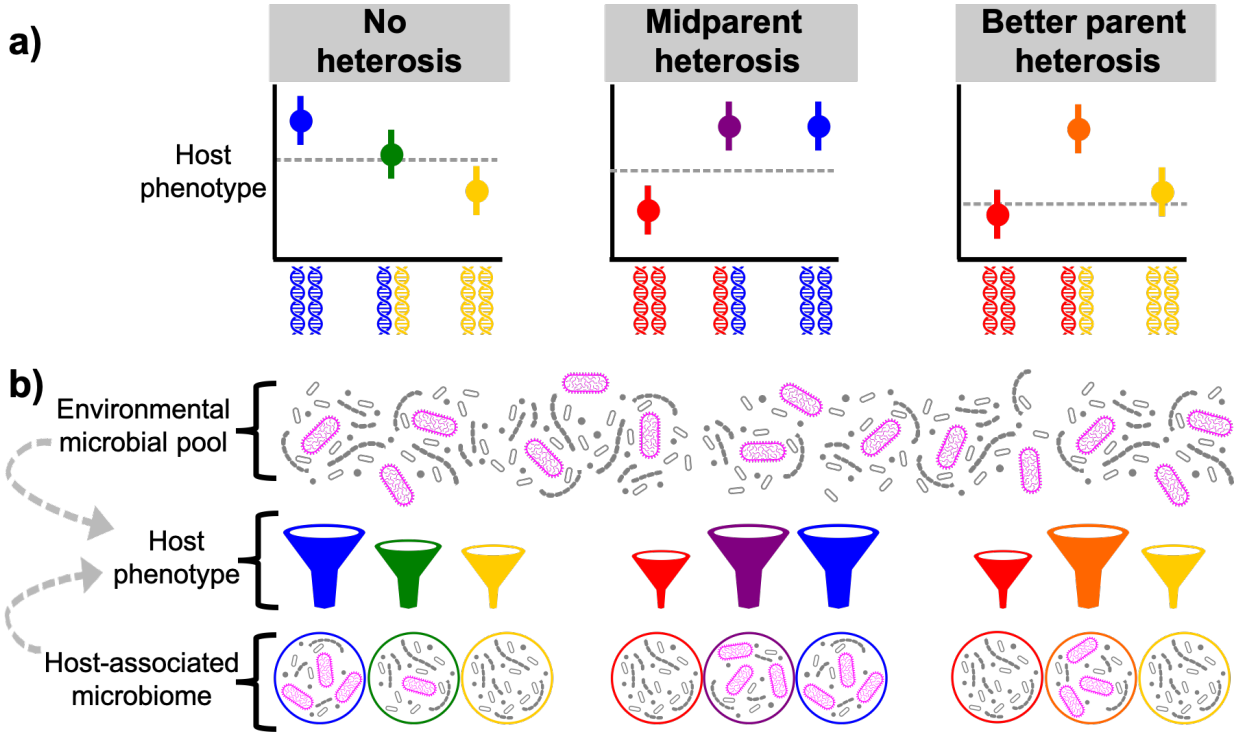

74
75 **Figure 1 |** Overview of heterosis and its hypothesized relationship to microbiome composition. **(a)**
76 Each panel depicts trait values for each of three genotypes: two inbred lines (left and right,
77 symbolized by blue, yellow, or red in the different panels) and their F_1 hybrid (center, symbolized
78 by green, purple, or orange). The dotted grey lines denote the midparent value, or the expected
79 trait value of the hybrid in the absence of heterosis. *Midparent heterosis* describes hybrid trait
80 values that deviate from the midparent value but are within the range of the parent line values.
81 *Better parent heterosis* describes hybrid trait values that are outside of the range of parental
82 values. **(b)** Host phenotype defines the habitat available to potential microbial colonizers from the
83 ambient community. Therefore, heterosis for traits that affect microbiome composition can result
84 in heterosis for microbiome composition itself (*e.g.*, relative abundance of the focal microbe
85 highlighted in pink). The dashed grey arrows represent the complication that microbes can alter
86 phenotypic expression in the host.
87
88 Although heterosis has been the subject of intense research for over 100 years, its
89 causes and mechanisms are still not completely understood. It likely involves various genetic
90 mechanisms including dominance, overdominance, and genic dosage, and affects a wide
91 variety of morphological and physiological traits (Birchler *et al.*, 2003; Flint-Garcia *et al.*, 2009;

92 Schnable & Springer, 2013). To the extent that host traits affecting microbiome composition
93 exhibit heterosis, microbiome composition itself could potentially do the same (Figure 1). So far,
94 however, exploration of the links between heterosis and plant microbiomes has been limited to
95 specific microbial groups and has excluded aboveground plant-microbe interactions. For
96 instance, maize hybrids are more likely than inbreds to be colonized by arbuscular mycorrhizal
97 fungi and by beneficial *Pseudomonas* strains that produce growth-promoting phytohormones
98 and protective antibiotic compounds in the rhizosphere (Picard *et al.*, 2004, 2008; Picard &
99 Bosco, 2005, 2006; An *et al.*, 2010).
100 Here, we investigate the effects of hybridization on maize leaf and rhizosphere
101 microbiomes. In maize, variation for leaf and rhizosphere microbiome composition has been
102 identified among diverse inbred lines (Peiffer *et al.*, 2013; Wallace *et al.*, 2018a; Walters *et al.*,
103 2018). The genes and traits underlying this variation are unknown, and hybrid offspring of these
104 or other inbred lines have not been fully characterized for microbiome content. Here, we focus
105 on linking host genotype to the microbiome, treating the phenotypic mechanisms as a “black
106 box”; this experiment was not optimized to identify the plant traits affecting microbial symbionts.
107 We used amplicon sequencing to quantify bacterial and fungal communities in eleven F_1 hybrids
108 and their parent lines, grown together in two experimental fields. We address the following
109 questions: (1) Do the microbiomes of maize hybrids differ consistently from those of inbred
110 lines? (2) Which microbiome features, if any, show heterosis within individual crosses? and (3)
111 Are patterns of microbiome heritability in F_1 crosses comparable to those of other complex
112 traits? The results are a significant step towards understanding the relationship between host
113 genotype and microbiome composition.
114

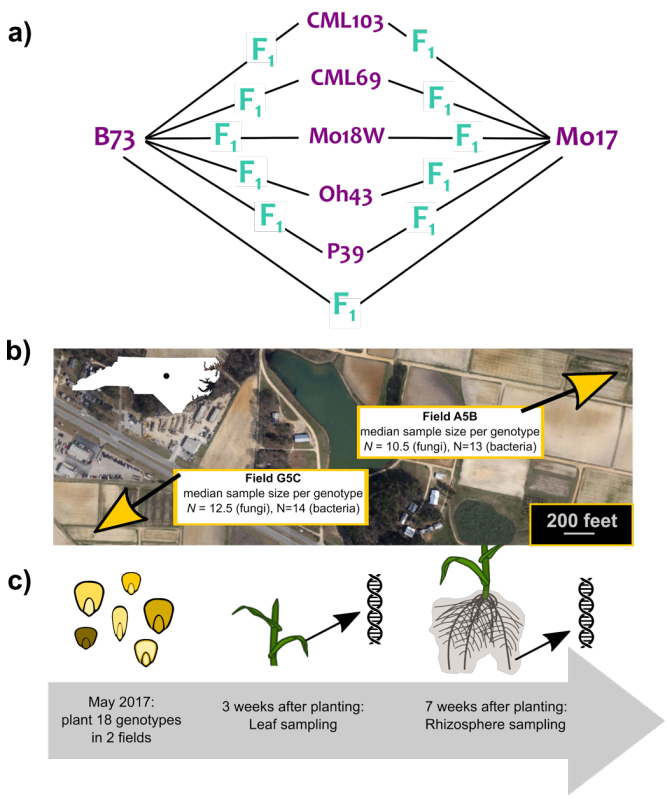

Figure 2 | Overview of experimental design. **(a)** Seven inbred lines and eleven F_1 hybrids (with B73 or Mo17 as the common maternal parent) were represented in our experiment. **(b)** Twenty to thirty replicates of each genotype were planted in randomized blocks in each of two fields at Central Crops Research Station, Clayton, NC, USA. Due to uneven germination and survival, the median sample size per genotype was slightly lower in Field A5B than in Field G5C; due to uneven sequencing of 16S and ITS amplicons and subsequent quality filtering, the median sample size was slightly lower for the fungal dataset than the bacterial dataset. Map data: Google (2019). **(c)** Leaf discs were collected from young plants three weeks after planting. Plants were uprooted seven weeks after planting (shortly before anthesis for most genotypes) and rhizosphere was collected and pooled from all root types to a depth of ~1 foot.

MATERIALS AND METHODS

Field experimental design

In May 2017, 18 maize genotypes were planted in a randomized design into two fields at Central Crops Research Station, Clayton, NC. The fields were 1.1 km apart and had similar soil types but different recent crop rotation histories and soil microbiota (Tables S1-S2).

131 The genotypes included the inbred lines B73 and Mo17; five additional inbred lines
132 selected from the founding members of the Nested Association Mapping population (Yu *et al.*,
133 2008); and 11 F_1 hybrids resulting from crosses of those lines to B73 and Mo17 (Figure 2a). For
134 all hybrids, either B73 or Mo17 was the maternal parent; for the B73xMo17 hybrid, B73 was the
135 maternal parent. We included B73 and Mo17 due to their importance as elite representatives of
136 the stiff-stalk and non-stiff-stalk heterotic groups and because they have high-quality reference
137 genomes that will facilitate deeper dissection of host genetic microbiome control (Jiao *et al.*,
138 2017; Sun *et al.*, 2018). The five additional inbred lines were chosen because they showed
139 highly divergent rhizosphere microbiome composition relative to each other and to B73 and
140 Mo17 in a previous study (Peiffer *et al.*, 2013). Some of these were sweetcorn lines or tropical in
141 origin; these groups are distinct from B73 and Mo17 in a wide variety of phenotypic traits
142 including root system architecture and phenology, all of which could potentially influence
143 microbiome composition. Thus, our study captured a wide range of maize genetic and
144 phenotypic variation; however, identifying the particular traits that caused any observed
145 microbiome changes was beyond the scope of this experiment.
146 Immediately prior to planting, kernels were soaked in 3% hydrogen peroxide for two
147 minutes to reduce surface-associated microbes and then rinsed in distilled water. One seed per
148 genotype was planted into each block, except for B73 and Mo17 which were planted an average
149 of 1.5 times per block. Twenty blocks of 18 or 20 individuals, randomized with respect to
150 genotype, were planted into adjacent rows within each field. However, the final sample sizes
151 were lower due to uneven germination, survival, and sequencing (Figure 2b).

152 Sample collection

153 Three weeks after planting, we sampled leaf tissue from all emerged plants for
154 microbiome analysis. We chose this early timepoint to ensure that sampling was completed
155 before the establishment of foliar diseases such as southern leaf blight, which sometimes arise
156 later in the season in these fields and which could potentially skew microbiome composition (but
157 see (Wagner *et al.*, 2020)). A standard hole punch and forceps (rinsed in 70% ethanol between
158 samples) were used to collect three discs evenly spaced from base to tip of the fourth leaf,
159 avoiding the midrib and any non-green tissue. Leaf discs were immediately placed into sterile
160 tubes and kept on ice until transfer to -20℃ for storage.
161 Seven weeks after planting, we uprooted plants for collection of rhizosphere soil. We
162 chose this timepoint so that our data would be comparable to the largest published maize

163 rhizosphere dataset available at the time (Peiffer *et al.*, 2013). This timepoint was originally
164 chosen based on the expectation that host genetic effects would accumulate in the rhizosphere
165 microbiome until the transition to flowering, while the roots were mostly a carbon sink (Peiffer &
166 Ley, 2013). Using a spade, we collected root crowns (~6" deep x ~18" wide) and shook them
167 until little or no bulk soil was falling from the roots. We then used ethanol-rinsed pruners to cut
168 all roots starting 2" below the top of the crown. All whorls of roots attached to the stem up to 6"
169 belowground were included in each sample; for large root systems that could not be grasped in
170 one hand, we instead cut all roots from one hemisphere of the crown to ensure that primary,
171 seminal, and crown roots would be represented in each sample. A variety of root system
172 properties likely differed among genotypes from different heterotic groups, or between hybrids
173 and inbreds; however, we conducted this experiment agnostic to the particular phenotypic traits
174 that affect microbiome composition. We therefore consider such genetic variation in root
175 morphology or physiology to be a possible underlying cause of any observed microbiome
176 variation, which would need to be verified through additional experimentation.
177 Cut roots were stored in a sterile plastic bag on ice until transfer to -20℃ for storage.
178 Rhizosphere collections were spread over four days (July 2nd-5th, 2017), with representatives of
179 all genotypes harvested from each field on each day so that collection date would not be
180 confounded with genotype or field (Figure S1). At time of rhizosphere sampling most plants had
181 transitioned to adult phase but were not yet flowering, with the exception of the sweet corn P39
182 which began anthesis during the collection period. We also collected bulk soil samples from the
183 four corners and approximate center of each field, approximately 8 cm below the surface. The
184 first ten soil samples were collected on July 4th, and sampling was repeated on July 5th for a
185 total of 20 samples.
186 We vortexed roots in 50 mL of 1x phosphate-buffered saline (PBS) at maximum speed
187 for 15 s to dislodge rhizosphere soil. The resulting suspension was poured through a sterile
188 100-micron stainless steel mesh into a sterile 50 mL tube, then centrifuged for 30 minutes at
189 1,600 x *g* to concentrate the rhizosphere soil. We then discarded the supernatant, resuspended
190 rhizosphere pellets in 1.5 mL 1x PBS, transferred them to sterile Eppendorf tubes, and
191 centrifuged them for 5 minutes at 10,000 x *g.* After discarding the remaining supernatant we
192 transferred rhizosphere pellets into storage at -80℃ until DNA extraction.
193 To determine whether this procedure affected downstream data collection and inference,
194 we tested the protocol on our bulk soil samples. Each bulk soil sample was divided into two
195 aliquots. We extracted DNA directly from one aliquot; to the other, we first applied the same
196 washing protocol that we used to separate rhizosphere from roots. Comparison of data from

197 washed and unwashed bulk soil samples indicates that the procedure may have resulted in
198 underestimates of alpha diversity and overestimates of beta diversity (i.e., resulted in loss of
199 some taxa and generated additional variation among samples) (Figure S2). Alternatively, alpha
200 diversity in bulk soils may have been inflated by the presence of dead cells or loose DNA that
201 were separated out by the washing process. Our data on rhizosphere microbiomes should be
202 interpreted with these caveats in mind.

203 DNA extraction

204 Prior to DNA extraction, we vortexed leaf discs at top speed for 10 seconds in 750 µL
205 sterile deionized water to remove dust and soil. Leaf discs were shaken dry and blotted on clean
206 paper towels, frozen at -80℃, and lyophilized. Freeze-dried leaf discs were randomly arranged
207 within 96-well plates and ground for 60 s at 25 Hz in a Retsch MM301 mixer mill. As a positive
208 control we included a mock microbial community in three wells (ZymoBiomics Microbial
209 Community Standard, Zymo Research, Irvine, CA, USA). We used the Synergy 2.0 Plant DNA
210 Extraction Kit (OPS Diagnostics, Lebanon, NJ, USA) to purify DNA, doubling the manufacturer's
211 recommended bead-beating time to improve lysis. Purified DNA was eluted in 30 µL of 1x TE
212 buffer (pH 8.0).
213 We used the MoBio PowerSoil htp-96 kit to extract DNA from rhizosphere and bulk soil
214 samples. Rhizosphere pellets were resuspended in 750 µL bead solution and transferred to 96-
215 well plates, with samples randomly arranged across plates. To improve lysis, samples were
216 subjected to two freeze-thaw cycles prior to extraction. Washed and unwashed bulk soil
217 samples (see above) were randomly distributed among the rhizosphere samples.

218 Amplicon library preparation and sequencing

219 As in previous work (Wagner *et al.*, 2020), we characterized bacterial and fungal
220 communities by sequencing the V4 region of the 16S rDNA gene and the ITS1 region of the
221 fungal rDNA gene, respectively. We amplified these barcoding genes using the primer pairs
222 515f/806r and ITS1f/ITS2, modified to include 3 to 6 random nucleotides upstream of the gene
223 primers to increase library complexity (Lundberg et al. 2013). A second PCR step added dual-
224 indexed Illumina adaptors to the amplicons. Barcoding genes were amplified in 10 µL reactions
225 that included 5 µL of 5Prime HotMasterMix (Quanta Bio, Beverly, MA, USA) and 0.4 µL of each
226 10 µM primer. For 16S-V4 amplification from leaf samples, we added 0.15 µL of PNA (100 µM)
227 to block amplification of host mitochondrial and chloroplast sequence (Lundberg *et al.*, 2013).

228 The template for the first PCR step was 1.5 μL of DNA extracted from leaf, rhizosphere, or mock
229 community samples; for the second PCR step, the template was 1 μL of the products from the
230 first step. Reaction conditions for ITS1 amplification were 2 minutes at 95℃; 27 cycles of 20 s at
231 95℃, 20 s at 50℃, and 50 s at 72℃; and a final 10 minutes at 72℃. Conditions for 16S-V4
232 amplification were identical except for an additional PNA-annealing step (5 s at 78℃) before
233 primer annealing at 52℃. The first PCR step included 27 cycles while the second included 8
234 cycles. PCR products from the first step were purified using 7 μL of magnetic SPRI bead
235 solution, two washes with 70% ethanol, and elution in 10 μL water. Finally, we pooled 1 μL of
236 each dual-indexed library, creating four separate pools (i.e., fungal and bacterial libraries for leaf
237 and rhizosphere samples). We used Blue Pippin (Sage Science Inc., Beverly, MA, USA) to
238 select fragments that were between 150 bp and 600 bp, and then combined the four pools at
239 equimolar concentrations. The final combined sample was sequenced on the Illumina HiSeq
240 2500 platform (250-bp paired-end reads).

241 Sequence processing and quality filtering

242 We used CUTADAPT v1.12 (Martin, 2011) to trim primers from raw sequences prior to
243 quality filtering. Using DADA2 v1.10.1 (Callahan *et al.*, 2016), we removed all reads with
244 ambiguous bases or more than 2 expected errors. Forward and reverse 16S reads were
245 truncated at 220 bp and 160 bp (respectively). We inferred error rates separately for 16S and
246 ITS data using $3x10^6$ bases, then de-replicated and de-noised reads to identify amplicon
247 sequence variants (ASVs). We removed chimeric ASVs using DADA2 and then used the RDP
248 classifier (Wang *et al.*, 2007) trained on the RDP training set (v. 16) and the UNITE database
249 (supplemented with *Zea* sequences) to assign taxonomy to bacterial and fungal ASVs,
250 respectively (Cole *et al.*, 2014; Nilsson *et al.*, 2019).
251 We discarded "non-usable" ASVs that could not be reliably identified at the kingdom
252 level and those identified as host sequences. Samples with <500 usable reads were excluded
253 from analysis. Within each sample we removed bacterial and fungal ASVs with less than 0.21%
254 and 0.185% relative abundance, respectively. These cutoffs were determined using the mock
255 community positive controls to identify relative abundance thresholds that minimized cross-
256 contaminant ASVs while retaining true positives and discarding as little data as possible. We
257 required ASVs to be observed at least 25 times in at least 5 samples to be considered
258 "reproducible"; all others were removed from the dataset (Lundberg *et al.*, 2012). Combined,
259 these quality filters reduced the number of bacterial ASVs from 8,958 to 753 and the number of

260 fungal ASVs from 4,863 to 501. However, 92.3% of the original bacterial data and 95.0% of the
261 fungal data were retained. The final number of observations for each sample was normalized,
262 centered, and used to control for sampling effort in downstream analyses.

263 Quantification of fungal abundance in the rhizosphere

264 For rhizosphere and soil samples, we used droplet digital PCR (ddPCR) to measure the
265 number of fungal 18S rRNA genes per unit of extracted DNA. We interpret this metric as an
266 estimate of the absolute abundance of fungi (*cf.* bacteria and other organisms) within the
267 community. DNA extracts were quantified using the PicoGreen dsDNA Assay Kit (Invitrogen,
268 Carlsbad, CA, USA) according to the manufacturer's instructions, and all samples were diluted
269 to a working concentration of 0.102 ng/uL. We used the FungiQuant assay to quantitatively
270 amplify the fungal 18S rRNA gene (Liu *et al.*, 2012). Each ddPCR reaction mixture contained 1
271 ng template DNA (9.8 uL of the diluted working solution), 5 uL of 2x Evagreen Probe Supermix
272 (Bio-Rad, Hercules, CA, USA), 0.1 uL of each 100nM primer (from 5' to 3', forward primer
273 GGRAAACTCACCAGGTCCAG and reverse primer GSWCTATCCCCAKCACGA), and
274 molecular-grade water to bring the reaction volume to 20uL. The reaction mixtures were loaded
275 into DG8 droplet generation cartridges along with 70uL of droplet generation oil for EvaGreen
276 assays, and the QX200 Droplet Generator was used to divide the mixture into droplets (Bio-
277 Rad). The droplets were then transferred to a T100 thermal cycler (Bio-Rad) for 10 minutes of
278 activation at 95℃; followed by 50 cycles of denaturation (30s at 95℃), annealing (60s at 55℃),
279 and elongation (30s at 72℃); and finally held at 4C until use. After amplification, the droplets
280 were transferred to the QX200 Droplet Reader and the QuantaSoft AP program (Bio-Rad) was
281 used to calculate the number of fungal 18S rRNA gene copies per ng of rhizosphere DNA.

282 Data analysis

283 Data analysis was performed in parallel for bacteria and fungi using R version 3.6.0 with
284 the packages phyloseq, vegan, DESeq2, tidyr, lme4, and lmerTest (McMurdie & Holmes, 2013;
285 Love *et al.*, 2014; Bates *et al.*, 2015; Kuznetsova *et al.*, 2017; Wickham, 2017; Oksanen *et al.*,
286 2019). Leaf and rhizosphere communities were analyzed in parallel. Raw sequence reads are
287 available at the NCBI Sequence Read Archive under Bioproject #PRJNA597058. Processed
288 data, metadata, and original code are available in a Zenodo archive (doi:
289 10.5281/zenodo.3596465).

290 ASV counts were normalized using the variance-stabilizing transformation from the
291 DESeq2 package (Love *et al.*, 2014). Before normalization we estimated alpha (within-sample)
292 diversity using the abundance-based coverage estimator (ACE) and Shannon metrics (Hughes
293 *et al.*, 2001). We quantified beta (between-sample) diversity by calculating the centroid for each
294 genotype in each field in multivariate space; then, using the function "betadisper" from the
295 package vegan (Oksanen *et al.*, 2019), we determined the distance of each sample to its
296 respective centroid.
297 **Comparing microbiome features of hybrid vs. inbred maize:** First, we investigated
298 whether the microbiomes of maize hybrids are distinct from those of inbreds. We modeled alpha
299 diversity (ACE and Shannon metrics) and beta diversity (distance to centroid) using separate
300 linear mixed models, with "category" (*i.e.*, either hybrid or inbred), field, and their interaction as
301 fixed effects. Normalized sequencing depth was included as a covariate. Genotype (nested
302 within category), block (nested within field), and plate (to control for batch effects) were included
303 as random-intercept terms. For rhizosphere samples, collection date was also included as a
304 random effect. ANOVA with Type III sums-of-squares and Satterthwaite's approximation of
305 degrees-of-freedom was used for statistical inference of fixed effects; likelihood ratio tests were
306 used for random effects.
307 To test whether hybrids and inbreds differed in overall community composition, we
308 conducted permutational MANOVA of Bray-Curtis dissimilarities, with hybrid/inbred category,
309 field, and their interaction as predictors. Sequencing depth and collection date were included as
310 nuisance variables. Finally, we fit negative binomial models to explore which microbial taxa
311 differed in relative abundance between hybrids and inbreds. ASV counts were modeled with
312 hybrid/inbred category as the predictor (Love *et al.*, 2014; McMurdie & Holmes, 2014). The
313 rarest taxa were excluded from this analysis: the threshold for inclusion was set at 10% of the
314 mean abundance. For example, the mean ASV count across the leaf fungal dataset was
315 14,057, so we included only ASVs that were observed at least 1,406 times. This reduced the
316 number of tests by 45% but still used 98.3% of the data. *P*-values from Wald tests were
317 adjusted to correct for multiple comparisons using the false discovery rate (Benjamini &
318 Hochberg, 1995).
319 **Testing for microbiome heterosis:** Next, we explored patterns of heterosis within
320 individual crosses for various microbiome features, including alpha and beta diversity (as
321 described above); overall community composition (summarized using the top 5 unconstrained
322 principal coordinates and the top 5 constrained axes of variation from a distance-based
323 redundancy analysis constrained on genotype); and variance-stabilized counts of ASVs. For

324 each feature we fit a linear mixed-effects model with the predictors field, sampling effort, batch
325 effects, and (for rhizosphere samples) collection date. The purpose of these models was not to
326 test for significance, but to derive residual trait values cleansed of these sources of noise; the
327 resulting residuals were then used to test for evidence of heterosis.
328 For each feature, we calculated the mean values of these residuals in the seven inbred
329 lines, from which we calculated the expected mid-parent values (assuming additive genetic
330 variance) for each hybrid. We then conducted two-sided *t*-tests of the null hypothesis that each
331 hybrid's microbiome trait value was equivalent to its respective mid-parent value (i.e., tests for
332 "mid-parent heterosis"; Figure 1a). In addition, we tested for "better-parent heterosis" using one-
333 sided *t*-tests to assess whether the hybrid value fell outside of the parental range. Finally, we
334 used linear regression to test for a relationship between microbiome heterosis (percent
335 deviation from expected mid-parent value) and average heterozygosity, estimated using
336 genome-wide SNP data from the maize HapMap v2 (Chia *et al.*, 2012).
337 **Effects of host relatedness on microbiome similarity within and between**
338 **environments:** To test whether the relationship between two host genotypes predicts the
339 similarity of their microbiomes, we calculated the Bray-Curtis dissimilarity between all pairwise
340 combinations of samples. Each pair of samples was classified according to the known
341 relationship (or lack thereof) between the two host genotypes. We fit a linear model of Bray-
342 Curtis dissimilarity with host-pair relationship as the predictor. The log-transformed absolute
343 difference in sequencing depth between samples was included as a covariate; host genotypes
344 and individual plant IDs were included as random intercept terms to account for these sources
345 of non-independence.
346 We used a similar approach to assess whether the microbiomes of hybrids and inbred
347 lines differed in their sensitivity to environmental variation. We modeled Bray-Curtis dissimilarity
348 between pairs of individuals with the same genotype using hybrid/inbred category,
349 within/between fields, and their interaction as predictor variables. The log-transformed absolute
350 difference in sequencing depth between samples was included as a covariate; the host
351 genotype and the two individual plant IDs were included as random intercept terms.
352 **Estimating heritability, general combining ability (GCA), and specific combining**
353 **ability (SCA) for microbiome composition:** Finally, we used ASReml-R software to estimate
354 GCA and SCA for key properties of hybrid microbiomes, including alpha diversity, beta diversity,
355 and the five major constrained and unconstrained axes of variation from the dbRDA described
356 above (Isik *et al.*, 2017). To estimate variance components for each of these microbiome
357 properties, we fit separate linear mixed-effects models for inbreds and hybrids with field,

358 sequencing depth, and collection date as fixed effects. For the inbred model, the random effects
359 included batch, block nested within field, genotype, and genotype-field interactions. For the
360 hybrid model, random effects included batch, block, female parent, male parent, the interaction
361 of each parent line with field, the interaction between the parent lines, and the three-way
362 interaction between the parent lines and field.

363 For hybrids, a diallel model was fit to the data, in which a single GCA effect was
364 estimated for each parent line, regardless of whether it was a male or female parent (Möhring *et*
365 *al.*, 2011). GCA variance is related to the variation of parental breeding values in hybrids and
366 additive variance was estimated as twice the GCA variance. SCA variance was calculated as
367 the variance component due to the interaction between the parent lines and represents variation
368 of dominance genetic effects, such as those that could lead to heterosis. The total genetic
369 variation was calculated as the sum of twice the GCA plus SCA; the total genotype-by-
370 environment (GxE) variation was calculated as the sum of the variance components from
371 interactions between each parent line and field (twice the GCA-field interaction plus the SCA-
372 field interaction variances). Narrow-sense heritability (h^2) was calculated as the additive
373 variance divided by the total phenotypic variation; broad-sense heritability (H) was calculated as
374 the total genetic variation (2*GCA + SCA) divided by the phenotypic variation. For inbreds, total
375 genetic variation and GxE were calculated using the variance components for genotype and
376 genotype-by-field interaction, respectively.

377 RESULTS

378 The final dataset included 501 fungal ASVs and 753 bacterial ASVs. The fungal dataset
379 comprised 481 leaf samples and 332 rhizosphere samples from a total of 547 individual plants,
380 with a median sampling effort of 19,266 observations per sample. The bacterial dataset included
381 502 leaf samples and 403 rhizosphere samples from 567 individuals (median sampling effort =
382 9,055 observations per sample). Plant survival differed between fields and genotypes, but the
383 median sample size ranged from N = 10.5 to N = 14 per genotype per field (Figure 2).

384 Leaf and rhizosphere communities differed substantially in diversity and composition
385 (Figure S3, Figure S4). Leaf communities were dominated by *Pantoaea*, *Entyloma*, and
386 *Golubevia* spp., while the most abundant taxa in the rhizosphere were *Ralstonia*, *Burkholderia,*
387 *Rhizobium, Entyloma,* and *Golubevia* (Table S3). Only 193 bacterial ASVs were observed in
388 both sample types; 260 bacterial ASVs were found only in leaves, whereas 290 were specific to
389 the rhizosphere. For fungi, 132 ASVs were specific to leaves, 196 were found only in the

rhizosphere, and 173 were found in both (Figure S4). Alpha diversity was higher in the rhizosphere than in leaves. For fungi, beta diversity was also higher in the rhizosphere, suggesting that belowground fungal communities may be more strongly influenced by microhabitat variation or stochastic processes (Figure S3c-d). This is consistent with the observation that community composition differed strongly between fields only for rhizosphere fungi (Figure S3a-b). As expected, rhizosphere communities were compositionally distinct from bulk soil (Figure S2); they also were relatively richer in fungi (Figure S5).

TABLE 1 | Permutational MANOVA of fungal and bacterial community composition in maize leaves and rhizosphere. *P*-values were generated from 999 permutations of Bray-Curtis dissimilarities among samples, which were calculated based on the matrix of variance-stabilized counts of amplicon sequence variants (ASVs). Results of an analogous test for variation among genotypes within hybrid/inbred categories are provided in Table S7.

		Bacteria			Fungi		
		R^2	pseudo-*F* test	*P*	R^2	pseudo-*F* test	*P*
Leaf	Category (inbred vs. hybrid)	0.002	$F_{1,499}$ = 1.16	0.25	0.004	$F_{1,478}$ = 2.03	0.006
	Field	0.021	$F_{1,499}$ = 10.85	0.001	0.075	$F_{1,478}$ = 39.77	0.001
	Category x Field	0.001	$F_{1,499}$ = 0.72	0.873	0.002	$F_{1,478}$ = 1.26	0.149
	Sequencing depth	0.014	$F_{1,499}$ = 6.97	0.001	0.027	$F_{1,478}$ = 14.61	0.001
Rhizosphere		R^2	pseudo-*F* test	*P*	R^2	pseudo-*F* test	*P*
	Category (inbred vs. hybrid)	0.013	$F_{1,398}$ = 7.09	0.001	0.011	$F_{1,329}$ = 5.37	0.001
	Field	0.134	$F_{1,398}$ = 73.03	0.001	0.234	$F_{1,329}$ = 118.68	0.001
	Category x Field	0.002	$F_{1,398}$ = 1.30	0.199	0.004	$F_{1,329}$ = 1.81	0.057
	Collection date	0.082	$F_{3,396}$ = 14.91	0.001	0.074	$F_{3,327}$ = 12.42	0.001
	Sequencing depth	0.044	$F_{1,398}$ = 23.86	0.001	0.038	$F_{1,329}$ = 19.03	0.001

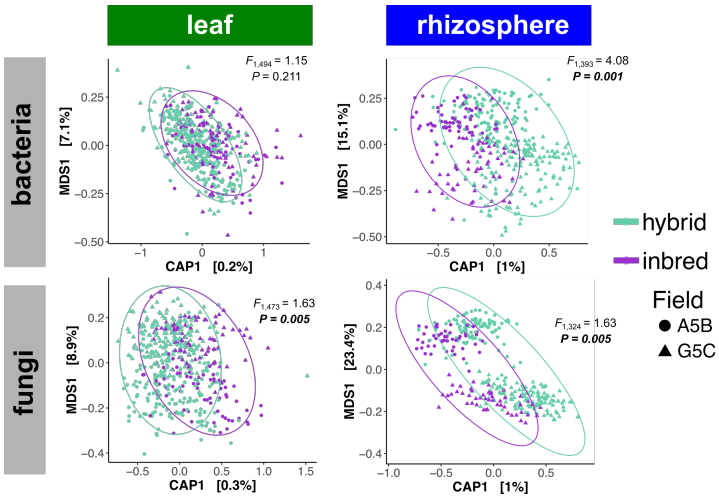

Figure 3 | Constrained distance-based redundancy analysis revealed that the microbiome composition of maize hybrids is distinct from that of inbred lines. Two axes of variation in community composition (ordination of Bray-Curtis dissimilarity) are plotted for bacterial and fungal communities in maize leaves and rhizosphere. The CAP1 axis was constrained to capture variation explained by inbred/hybrid category; MDS1 was the dominant unconstrained axis of variation. ANOVA-like permutation tests were performed to assess statistical significance of the constrained axis.

Microbiome composition differs between maize hybrids and inbred lines

First, we investigated whether hybrids, as a group, differed from inbreds in microbiome diversity and composition. For bacteria and leaf-associated fungi, we found no consistent difference between these groups in either alpha diversity or beta diversity (Table S4). In contrast, fungal communities in the rhizospheres of hybrid plants had higher alpha diversity (within-sample species richness and evenness) and lower beta diversity (among-individual variability) relative to inbreds (Tukey's HSD, $P < 0.05$).

Hybrids' microbiomes were primarily distinguished from those of inbred plants not by alpha or beta diversity, but by overall community composition (Table 1). Distance-based redundancy analysis (ordination of Bray-Curtis dissimilarity, constrained to emphasize variation explained by hybrid/inbred category) revealed that microbiomes of maize hybrids clustered with those of other hybrids, apart from those of inbreds (Figure 3). We confirmed this observation using permutational MANOVA; hybrid/inbred category predicted the composition of leaf-associated fungal communities and rhizosphere bacterial and fungal communities (ADONIS, all $P<0.01$). This differentiation was strongest in the rhizosphere, explaining about 1.6% of the overall variation (compared to <1% in leaves). Using negative binomial models, we identified 18

424 bacterial and fungal ASVs that were differentially abundant in the rhizosphere of hybrid versus
425 inbred hosts (Figure 4).

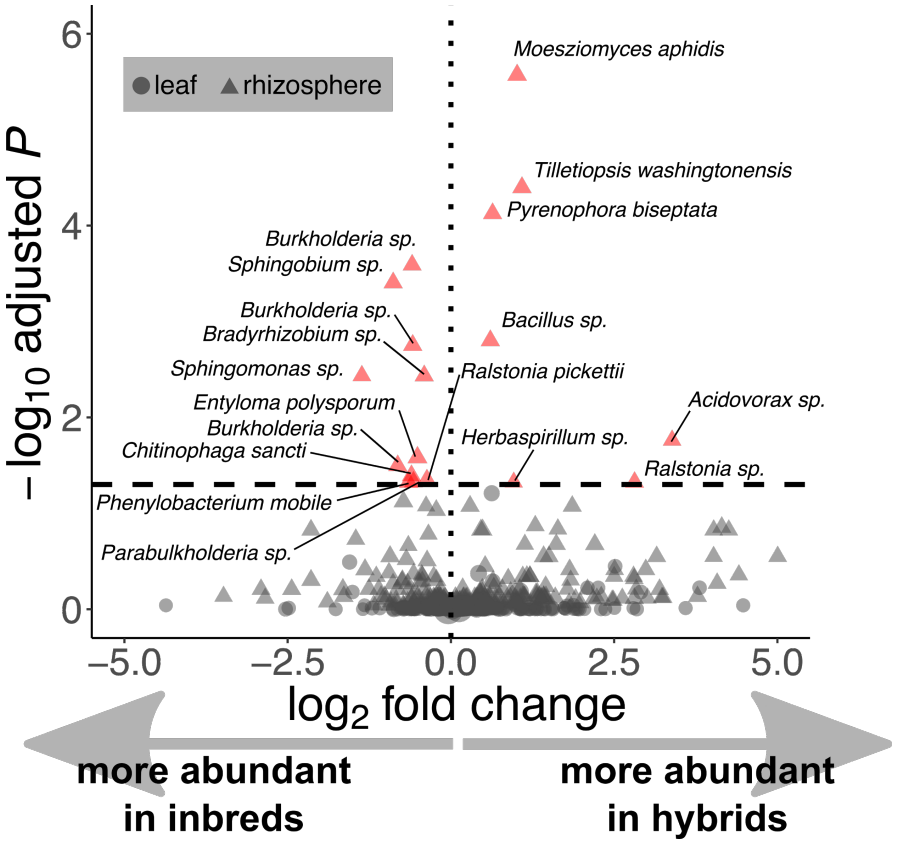

426
427

428 **Figure 4 | Diverse bacterial and fungal taxa were enriched or depleted in the rhizosphere of maize**
429 **hybrids relative to inbred lines.** For this analysis, data from the two fields were pooled. Each point
430 represents one ASV, with point size scaled by the relative abundance of that taxon. FDR-corrected *P*-
431 values from Wald tests of negative binomial models of taxon counts are plotted against the estimated
432 effect sizes from the same models. Red points reflect taxa that were significantly associated with host
433 hybrid/inbred category (FDR < 0.05). ASVs are labeled as the closest-matching species based on
434 comparison to the NCBI sequence database using BLAST. One leaf ASV (*Microdochium sorghi*) is
435 omitted to improve figure clarity; it was strongly enriched in hybrids.

436 Patterns of heterosis in microbiome features

437 Next, we tested which microbiome features, if any, showed evidence of heterosis within
438 individual crosses. These features included community-level metrics of alpha and beta diversity
439 (*i.e.,* Shannon, ACE, distance-to-centroid) and composition (the top 5 constrained and
440 unconstrained axes of variation from distance-based redundancy analysis; Figure 5b). We used

441 *t*-tests to assess whether these microbiome features deviated from the midparent expectation
442 for each hybrid, using a significance threshold of FDR < 0.05 (Figure 1). We note that
443 historically, the term "better-parent" heterosis describes cases in which the hybrid has higher
444 values of a desirable trait or lower values of an undesirable trait relative to both parents (Flint-
445 Garcia *et al.*, 2009). Because the function and value of these microbiome traits (if any) are
446 unknown, we use this term to refer to cases in which hybrid trait values are higher than both
447 parents or lower than both parents (Figure 1a).
448 Heterosis for alpha and beta diversity was detected in a few crosses, but the most
449 frequently heterotic microbiome features were the axes of variation in community composition.
450 Both midparent and "better-parent" heterosis were particularly common in the dbRDA axes that
451 were constrained by host genotype (Figure 5a), which is consistent with these axes capturing
452 the heritable components of microbiome composition. More microbiome features displayed
453 heterosis in the rhizosphere than in leaves, which is consistent with the overall stronger
454 differences between hybrids and inbreds observed previously (Figure 3). Linear regressions
455 revealed that genome-wide heterozygosity did not reliably predict the strength of microbiome
456 heterosis, quantified as the percent deviation from expected midparent values of microbiome
457 features (Figure S6). Heterozygosity was positively associated with heterosis only for the
458 bacterial MDS1 in the rhizosphere (R^2 = 0.53, P=0.03). For bacterial CAP1 and fungal beta
459 diversity, the relationship was inverse. Most frequently, however, we found no significant
460 relationship, although this could reflect low statistical power due to the small number of hybrids
461 tested (N=11).
462 We also tested for heterosis of individual ASVs using FDR-corrected *t*-tests of their
463 variance-stabilized abundances. In most hybrids, most ASVs did not deviate from the midparent
464 expectation (Figure S7a). However, 40% of rhizosphere fungal ASVs showed evidence of
465 heterosis in at least one cross, as did 20% of leaf-associated fungal ASVs, representing a wide
466 diversity of classes (Figure S7b; Table S5). For bacterial ASVs, the rates of heterosis in the
467 rhizosphere and leaf were 35% and 17%, respectively. The prevalence of ASV heterosis varied
468 among hybrids, ranging from 27% of the tested fungal ASVs in the B73xP39 rhizosphere, to
469 5.1% of the tested bacterial ASVs in the B73xMo17 rhizosphere (Figure S7a). The most
470 strongly heterotic fungal ASV (showing "better-parent" heterosis most frequently) belonged to
471 the yeast *Moesziomyces aphidis*, which was enriched in the rhizospheres of six hybrids relative
472 to both of their inbred lines (Figure S8). Two bacterial ASVs in the rhizosphere (*Pseudonocardia*
473 sp. and *Sphingomonas* sp.) and one in the phyllosphere (*Acinetobacter* sp.) each showed
474 "better-parent" heterosis in five hybrids (Figure S8).

For both bacteria and fungi, the second constrained axis of rhizosphere variation (CAP2) was the most frequently heterotic microbiome property; hybrid values of bacterial CAP2 exceeded both parental values for all 11 crosses (Figure 5). To obtain a biological interpretation of CAP2, we identified the top 10% of ASVs with the strongest loadings on this axis (Table S6). These included 13 of the ASVs that were differentially abundant between hybrids and inbred lines (Figure 4), including three *Burkholderia* ASVs. Additional rhizosphere ASVs with strong influences on this axis included three more *Burkholderia* ASVs, two *Nitrospira* ASVs, and four ASVs from the family Rhizobiaceae.

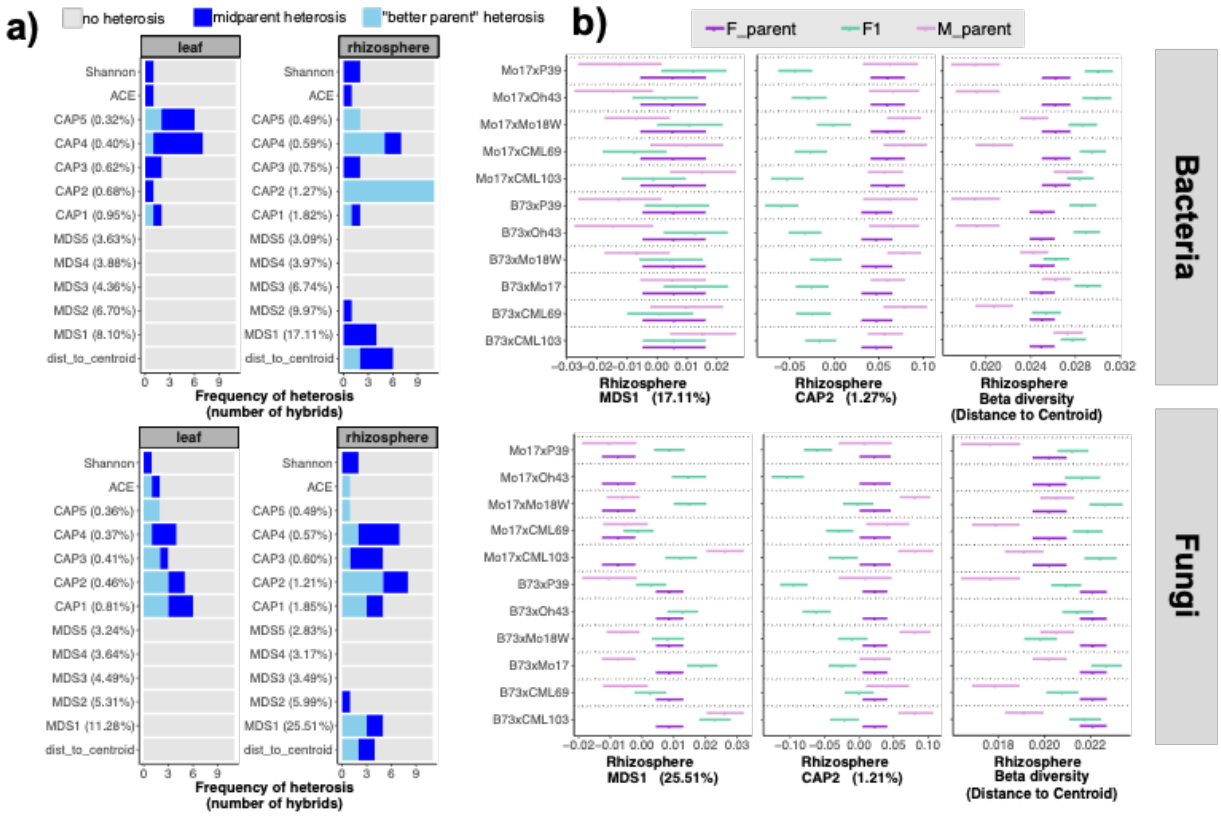

Figure 5 | Multiple microbiome properties show evidence of heterosis in maize leaves and rhizosphere for both bacteria (top of each panel) and fungi (bottom of each panel). We calculated the values of select microbiome features in maize hybrids, after controlling for field, sequencing depth, and batch effects; then, we used *t*-tests to compare hybrid trait values to the mid-parental trait values as illustrated in Figure 1. *P*-values were adjusted to correct for multiple tests using the false discovery rate (Benjamini & Hochberg, 1995). **(a)** Heterosis was more common for some microbiome properties than others. This difference is especially stark for community composition, summarized using the top 5 constrained and unconstrained axes of variation resulting from distance-based redundancy analysis. The constrained axes (abbreviated

494 “CAP” for Constrained Analysis of Principal Coordinates) capture the microbiome variation that is
495 associated with host genotype; the unconstrained axes (abbreviated “MDS” for Multidimensional
496 Scaling) capture the dominant axes of remaining variation. The percentage of the overall
497 community composition explained by each CAP or MDS axis is specified on the *y*-axis. **(b)**
498 Patterns of heterosis are illustrated for two axes of variation in rhizosphere community
499 composition, as described for panel (a), and for rhizosphere beta diversity (distance to centroid),
500 which quantifies within-group/among-individual variation in community composition. Points
501 represent least-squares mean values +/- 1 s.e.m.

502 Patterns of microbiome heritability in F_1 crosses

503 Finally, we investigated general patterns of microbiome heritability in this set of maize
504 crosses. In particular, we (1) partitioned variance in community composition among genotypes
505 within hybrid/inbred categories; (2) compared microbiome similarity of pairs of genotypes with
506 differing levels of relatedness; (3) tested whether the microbiomes of hybrid and inbred maize
507 were equally influenced by environmental variation; and (4) investigated the relative importance
508 of additive versus heterotic components of genetic variation for shaping hybrid microbiomes.
509 First, we used permutational MANOVA to test for host genetic variation among inbred
510 lines and among hybrids for whole-community composition. Host genotype contributed 4-8% of
511 the variation in overall community composition for both bacteria and fungi, in both leaves and
512 rhizosphere (Table S7). Alpha and beta diversity also varied among host genotypes, but not as
513 consistently as community composition. For instance, host genotype affected alpha diversity
514 and distance to centroid (*i.e.,* among-individual variation within genotypes); but almost
515 exclusively in the rhizosphere (Table S4).
516 Next, to assess how relatedness affects microbiome similarity, we modeled Bray-Curtis
517 dissimilarity between pairs of samples as a response to host-genotype-relationship using
518 ANOVA. Overall, host-genotype-relationship had a stronger effect on rhizosphere microbiome
519 dissimilarity than leaf microbiome dissimilarity (Figure 6a). Bacterial rhizosphere composition
520 differed more between pairs of hybrids (regardless of their relatedness) than between pairs of
521 inbreds; the opposite was true in leaves. We found no evidence that hybrids’ microbiomes are
522 more similar to those of their maternal inbred than to their paternal inbred; in fact, for leaf-
523 associated bacteria, the opposite was true. Similarly, hybrid microbiomes were equally
524 dissimilar to those of their half-siblings regardless of whether the female or male parent was
525 shared (Figure 6a).

526 Third, we tested whether genotype-by-environment (GxE) interactions are more
527 prominent for inbred microbiomes than hybrid microbiomes, as they are for many plant traits
528 (Lewis, 1954; Griffing & Zsiros, 1971; Blum, 2013; Zanewich *et al.*, 2018) (but see (Li *et al.*,
529 2018)). We found that pairs of siblings from hybrid genotypes had *less* similar rhizosphere
530 microbiomes than pairs of siblings from inbred genotypes, both within fields and between fields
531 (Figure 6b). In addition, fungal load in the rhizosphere was stable across fields for inbreds, but
532 not hybrids (Figure S5). For leaf microbiomes, however, there was no difference in sibling-pair
533 dissimilarity between inbreds and hybrids. The variance components contributed by Genotype
534 and GxE supported these findings. For many leaf microbiome traits, G/GxE was equal between
535 hybrids and inbreds; for others (particularly fungal traits) it was higher in hybrids, and for others
536 (particularly bacterial traits) the opposite was true (Figure S9a).
537 Last, we investigated whether hybrid microbiomes were influenced more by general
538 combining ability (GCA; the average trait values of the two parent lines, mostly involving additive
539 gene effects) or specific combining ability (SCA; the interaction between the two parent lines,
540 involving synergistic or heterotic effects). Using this method we detected moderate heritability
541 for a variety of leaf microbiome features, but no heritability for rhizosphere microbiomes. For
542 both fungi and bacteria, narrow-sense heritability (h^2) was much higher among inbred lines than
543 among hybrids (Figure S9b). For hybrids, comparison of SCA and GCA revealed that for
544 multiple axes of leaf microbiome variation, broad-sense heritability was considerably higher than
545 h^2 (Figure S9c). This indicates that leaf microbiomes, in particular, were shaped by specific
546 combinations of parental genotypes (*i.e.,* heterotic or synergistic effects) beyond the general
547 combining ability (additive effects) of those parents.

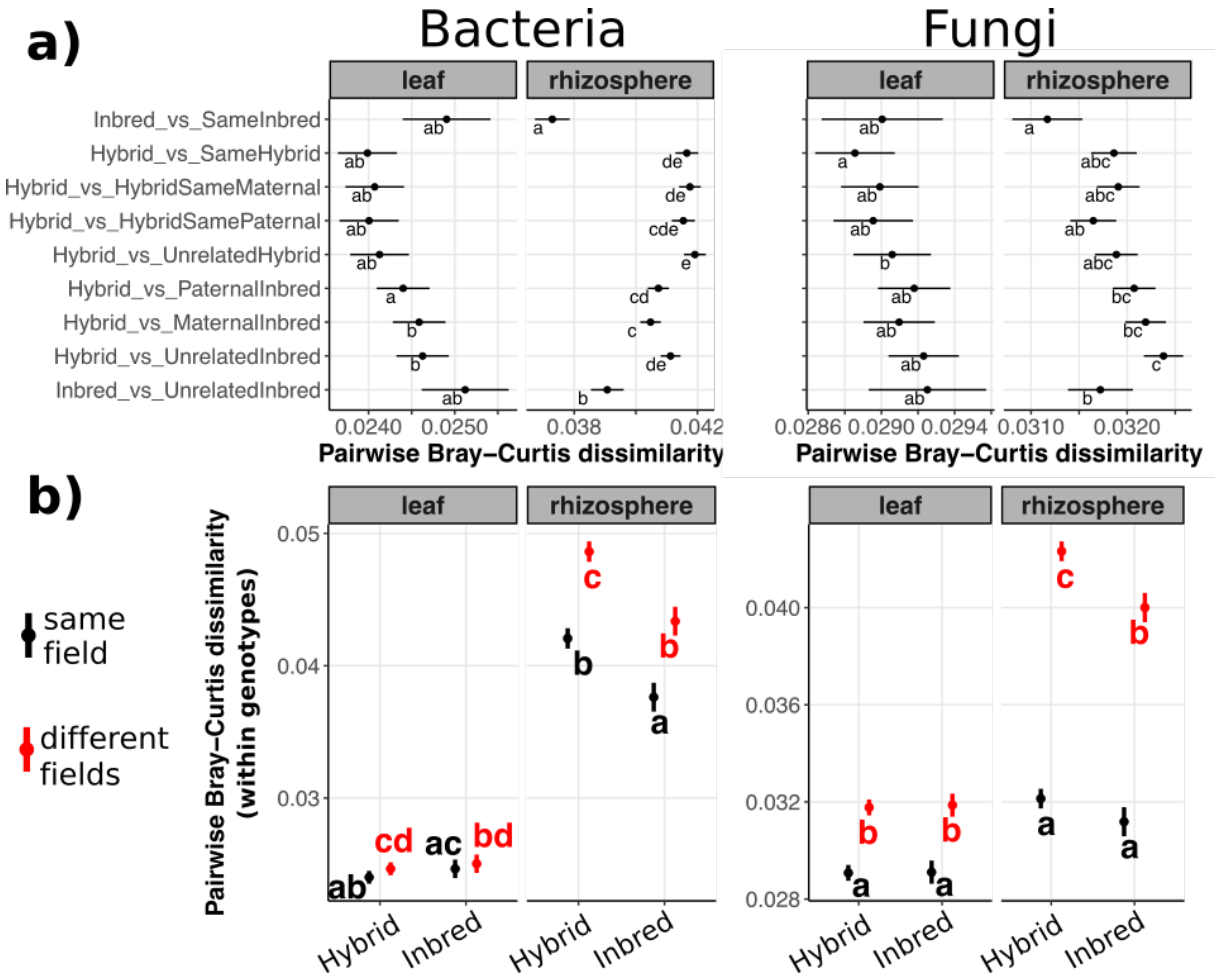

Figure 6 | Host relatedness affects dissimilarity between pairs of microbiomes. (a) Bray-Curtis dissimilarity (horizontal axis) was calculated for each pair of samples, each of which was categorized according to the relationship between the two samples' host genotypes (vertical axis). All sample pairs were from individuals in the same field. We used ANOVA to test the response of Bray-Curtis dissimilarity to "host-pair-relationship"; the log absolute value of the difference in sequencing depth between the samples was included as a nuisance variable. Least-squares mean dissimilarity values from this model are shown +/- 1 s.e.m. Non-overlapping sets of letters indicate post-hoc Tukey's Honest Significant Differences. **(b)** Pairs of rhizosphere samples from inbred genotypes were more similar to each other in composition than pairs of samples from hybrid genotypes. Bray-Curtis dissimilarity was modeled as a function of "inbred/hybrid category", "within vs. between field", and their interaction; least-squares means are plotted as described in (a).

DISCUSSION

Understanding patterns and mechanisms of microbiome heritability is critical to understanding the evolution of host-microbiome symbiosis in both natural and human-directed systems. Here we demonstrate that microbiome diversity and composition display some of the same patterns as other complex plant traits within F1 crosses. In general, leaf and rhizosphere microbiomes of hybrid maize differ reliably from those of inbred maize lines, much like performance-related traits such as height and yield (Flint-Garcia *et al.*, 2009). Within crosses, we detected evidence for heterosis of a variety of microbiome features, including beta diversity and several orthogonal axes of community composition (Figure 5).

Overall, effects of hybridization (and of host genotype more generally) were stronger in the rhizosphere than in the leaves. The reasons for this are unclear. One possible explanation is that the difference in sampling time (3 weeks after planting for leaves, 7 weeks for rhizosphere) allowed more time for deterministic effects of host genotype to shape rhizosphere communities, whereas the leaf microbiome reflected more of the stochastic variation that contributes to initial community assembly (Maignien *et al.*, 2014). It is important to note that in our study, the observed differences between leaf and rhizosphere communities reflect not only the distinction between aboveground and belowground organs, but also differences in abiotic environment and in plant developmental stage that correspond to the two timepoints. Maize leaf microbiomes change drastically over the growing season (Wagner *et al.*, 2020). Nevertheless, studies from diverse plant species confirm that leaf and rhizosphere microbiomes are reliably distinct (Coleman-Derr *et al.*, 2016; Wagner *et al.*, 2016; Wallace *et al.*, 2018b). In maize, individual leaves can senesce within weeks, especially early in development; in contrast, much of the root system remains active throughout the plant's lifespan (Fusseder, 1987). Thus, maize leaves are generally more transient habitats for microbes than maize rhizosphere. However, the same is true for the perennial forb *Boechera stricta*, in which host genotype effects were stronger in leaves than in roots (Wagner *et al.*, 2016). One potential explanation for this opposite result is that maize forms partnerships with mycorrhizal fungi, while (like other mustards) *B. stricta* does not; this hints at fundamental differences in mechanisms of interaction with belowground microbes.

In this study, host genotype and its interaction with environment explained between 4-8% of the overall variation in microbiome composition (Table S3). This is a high proportion relative to other studies of host genetic microbiome control, but low relative to studies of other maize traits; flowering time and resistance to various diseases often have heritabilities above

594 80% (Robertson *et al.*, 2006; Buckler *et al.*, 2009). However, this may be an underestimate of
595 the true importance of host genotype. If only a subset of the microbiome is actually responsive
596 to host variation, then using the entire community as a response variable is likely diluting the
597 host genotype signal. In support of this possibility, some studies, including in maize, have found
598 that heritability of microbiome functional potential (*i.e.,* metagenome content) is higher than the
599 heritability of taxonomy-based microbiome features such as those used in our analysis
600 (Lemanceau *et al.*, 2017; Wallace *et al.*, 2018a).
601 Maize is well-known for the strength of heterosis in intraspecific crosses, and our results
602 indicate that this phenomenon can be seen within leaf and rhizosphere microbiomes. However,
603 not all maize crosses are equally heterotic, either for yield or for the underlying traits (Flint-
604 Garcia *et al.*, 2009; Guo *et al.*, 2019). This, too, was evident in our microbiome data (Figure 5;
605 Figure S7), although we found no consistent relationship between heterozygosity (estimated
606 from genome-wide SNP data) and microbiome heterosis (Figure S6). However, with only 11
607 crosses included in our study, an explicit test for a relationship between the extent of
608 microbiome heterosis and the extent of heterosis for other phenotypic traits was beyond the
609 scope of this work. One hurdle to addressing this question is the general lack of knowledge
610 about which plant traits cause changes in the microbiome. Mutant and transgenic studies in
611 Arabidopsis have demonstrated that properties of the leaf cuticle affect microbial colonization
612 (Bodenhausen *et al.*, 2014; Ritpitakphong *et al.*, 2016), and that physiological traits such as
613 hormone signalling and defensive secondary chemistry influence the root and rhizosphere
614 microbiomes (Bressan *et al.*, 2009; Lebeis *et al.*, 2015). However, it is unknown whether the
615 same traits are involved in shaping the maize microbiome. An additional complication is the fact
616 that the microbiome can, in turn, affect phenotypic expression in the host plant (O'Brien *et al.*;
617 Panke-Buisse *et al.*, 2017; Berg & Koskella, 2018) as well as the relationship between
618 phenotype and yield (Wagner *et al.*, 2014; Chaney & Baucom, 2020). For these reasons, careful
619 experimentation—not just simultaneous measurement of plant traits and microbiome features—
620 will be needed to clarify the phenotypic links between heterozygosity and microbiome heterosis
621 (Figure 1).
622 Although no comparable studies are currently available, we expect that other sets of
623 maize genotypes, and indeed other plant species, could show different effects of hybridization
624 on the microbiome. A comparison to plant species that display outbreeding depression rather
625 than heterosis would be particularly interesting. Evidence from animal systems suggests a
626 potential role for the microbiome in speciation. Crosses between two subspecies of house mice
627 (*Mus musculus*) result in hybrid offspring with reduced fertility and gut microbiomes that diverge

628 from both parent subspecies (Wang *et al.*, 2015), while lethality of hybrids between species of
629 *Nasonia* wasps can be attributed to a disordered microbiome (Brucker & Bordenstein, 2013). To
630 our knowledge, however, our study is the first to investigate whole microbiome composition in
631 true intraspecific crosses of any organism. More data is needed from similar experiments,
632 particularly in additional plant species that vary in mating system.
633 Notably, the lines used in our study are known to vary in phenology and developmental
634 trajectories (Buckler *et al.*, 2009). To the extent that the phenotypic traits affecting the
635 microbiome vary over development, this variation may be one of the mechanisms underlying the
636 observed microbiome differences among genotypes. This is more likely to be the case for
637 rhizosphere samples (collected ~7 weeks after planting) than for the leaf samples (collected ~3
638 weeks after planting), because genetic variation for phyllochron is quite low in maize (Van
639 Esbroeck *et al.*, 2008). A weekly time-series revealed genotype-by-timepoint interactions
640 influencing rhizosphere microbiome composition throughout the growing season; however, the
641 strength of this interaction was minor compared to the effects of location and timepoint (Walters
642 *et al.*, 2018). Interestingly, that study revealed a qualitative change in maize microbiomes which
643 occurred in all genotypes between weeks 7 and 8 of development: a bloom of *Pseudomonas*,
644 which increased suddenly in relative abundance from ~3% to over 44%. This bloom was
645 observed only in rhizosphere (not in bulk soil) and persisted for the rest of the growing season.
646 In our study, *Pseudomonas* comprised 2.3% of the rhizosphere community on average,
647 consistent with the results of Walters *et al.* The abundance of *Pseudomonas* varied among
648 genotypes but never averaged more than 3.4% (Figure S10). This suggests that at the time of
649 sampling, no genotype had progressed to the developmental stage that triggers the
650 *Pseudomonas* bloom. Of course, this does not rule out the possibility that more subtle
651 differences in microbiome composition were driven by plant development; however, there is no
652 evidence that phenology was a dominant driver of the observed microbiome differences among
653 genotypes.
654 Some of the taxa that distinguish hybrids and inbreds (Figure 4) have been linked to
655 positive or negative effects on plant health. For example, *Burkholderia* spp. have been reported
656 to improve growth and stress resilience in diverse plants including maize (Bevivino *et al.*, 2000;
657 Mitter *et al.*, 2013), and a sizeable minority of maize-associated *Burkholderia* strains appear to
658 be nitrogen fixers (Perin *et al.*, 2006). Although maize does not make the root nodules that are
659 central to rhizobial symbiosis in legumes, strains of *Bradyrhizobium* have been shown to
660 increase aboveground biomass in maize by up to 20% (Prévost *et al.*, 2012) and can fix
661 nitrogen while free-living (Smercina *et al.*, 2019). The yeast-like fungus *Tilletiopsis*

662 *washingtonensis* produces antifungal metabolites and has shown promise as a biocontrol agent
663 (Urquhart, 1994; Urquhart & Punja, 2002). One ASV identified as *Microdochium sorghi* was
664 strongly enriched in the leaves of hybrids relative to inbreds. This fungus can cause zonate leaf
665 spot disease in maize, although it more commonly infects sorghum (De León, 1978; Korsman *et*
666 *al.*, 2012); however, no symptoms were apparent in the plants in this experiment. Interestingly, a
667 recent study in *Populus* also found an enrichment of foliar fungal pathogens in an interspecific
668 hybrid relative to one of the parent species (Cregger *et al.*, 2018).
669 Without additional data, however, the observed differences in microbiome composition
670 between hybrids and inbreds cannot be reliably translated into differences for microbiome
671 function and/or plant health. This reflects the limitations of the amplicon-sequencing approach.
672 Due to poor taxonomic resolution and a general lack of knowledge about the biology of many
673 microbial taxa, function cannot be reliably inferred from this type of data. Therefore, different
674 approaches are needed to draw conclusions about the importance of microbiome heterosis for
675 community and host function. The true functional consequences of microbiome heterosis would
676 be most clearly assessed by directly manipulating microbiomes and measuring the effects on
677 host phenotype. This approach would also inform us about the direction of causality in the
678 microbiome-heterosis relationship. In this study, we manipulated host genotype and measured
679 the effects on microbial communities; however, given the abundant evidence that plant
680 microbiomes can drastically affect their hosts, the observed effects on the microbiome could
681 feed back and contribute to heterosis of other plant traits. Is microbiome heterosis a
682 meaningless by-product of host hybridization? Or is it a contributing mechanism of hybrid vigor
683 itself? These questions could be addressed using synthetic microbial communities,
684 reinoculation, or soil-conditioning experiments (Ponsford *et al.*; Panke-Buisse *et al.*, 2015;
685 Vorholt *et al.*, 2017). These important next steps will help to clarify the role of plant-associated
686 microbes in hybrid vigor.

687 ACKNOWLEDGEMENTS

688 We thank G. Marshall, S. Sermons, and J. Torres for assistance with field and lab work. We
689 thank Cathy Herring and the staff at NC Central Crops Research farm for managing the field
690 trials. We thank L. Burghardt and D. Leopold for valuable comments on earlier drafts of the
691 manuscript. All sequencing was done by the North Carolina State University Genomic Sciences
692 Laboratory (Raleigh, NC, USA). M.R.W. was supported by a NSF National Plant Genome
693 Initiative Postdoctoral Research Fellowship in Biology (IOS-1612951) and a NSF EPSCoR RII

Track-1 grant (OIA-1656006). This work was funded by a NCSU Plant Soil Microbial Community Consortium grant to J.B.H. and M.R.W.

AUTHOR CONTRIBUTIONS

MRW, PBK, and JBH planned and designed the research. MRW, JHR, and PBK performed experiments and conducted fieldwork. MRW and JBH analyzed data. MRW wrote the manuscript with edits from PBK and JBH.

SUPPLEMENTARY INFORMATION

TABLE S1 | Soil types and crop rotation histories of the two fields at Central Crops Research Station, Clayton, NC, USA. The fields were 1.1 km apart.

Field	**Soil**	**Rotation** (2014-2017)
A5B	Wagram loamy sand	Squash > Soybean > Corn > Corn
G5C	Wagram loamy sand	Corn > Tobacco > Cucumber > Corn

TABLE S2 | 49 plant-colonizing ASVs were differentially abundant between the bulk soils of the two fields. The log2FoldChange indicates the direction and magnitude of differential abundance, with positive/negative values describing ASVs that had higher relative abundances in bulk soils of field A5B/G5C, respectively. Column lfcSE notes the standard error of the estimated log2FoldChange. Taxa that could not be identified at the genus level are indicated with parentheses. The "Colonizes" column indicates whether the ASV was observed in leaf samples, rhizosphere samples, or both.

log2FoldChange	lfcSE	ASV_ID	Kingdom	Genus	Colonizes
24.69	3.02	fASV_398	Fungi	Epicoccum	leaf
23.17	3.16	fASV_148	Fungi	(Sordariales)	leaf
22.84	2.99	bASV_522	Bacteria	Ralstonia	leaf
22.79	2.89	bASV_159	Bacteria	Dyella	both
11.51	2.98	fASV_131	Fungi	(Sordariales)	both
10.77	1.78	fASV_489	Fungi	(Cantharellales)	rhizosphere
9.51	2.61	fASV_132	Fungi	(Sordariales)	leaf
8.51	2.31	fASV_339	Fungi	Poaceascoma	both
8.41	1.74	fASV_289	Fungi	Exophiala	leaf
7.93	2.04	bASV_437	Bacteria	Gaiella	leaf
7.81	2.17	fASV_231	Fungi	(Mortierellales)	leaf
7.72	2.58	fASV_451	Fungi	Corynespora	rhizosphere
7.6	1.73	bASV_274	Bacteria	(Xanthomonadaceae)	rhizosphere
7.42	2.1	fASV_218	Fungi	Acremonium	both
7.32	1.88	fASV_124	Fungi	(Sordariomycetes)	rhizosphere
7.24	2.97	fASV_486	Fungi	Mortierella	both
6.97	2.01	bASV_165	Bacteria	Rhodanobacter	both
6.96	2.55	bASV_678	Bacteria	Tumebacillus	rhizosphere
6.79	2.07	fASV_202	Fungi	(Ascomycota)	both
6.72	2.25	fASV_417	Fungi	(Tremellales)	both
6.57	2	bASV_737	Bacteria	Tumebacillus	rhizosphere
6.5	2.35	bASV_610	Bacteria	Burkholderia	rhizosphere
6.49	2.46	fASV_384	Fungi	(Fungi)	rhizosphere
6.48	2.17	bASV_163	Bacteria	Rhodanobacter	leaf
6.36	1.71	bASV_446	Bacteria	Gaiella	rhizosphere
6.22	1.99	bASV_553	Bacteria	Massilia	leaf
6.2	2.46	fASV_290	Fungi	Exophiala	rhizosphere
5.99	1.76	fASV_167	Fungi	Chloridium	both
5.92	1.99	bASV_442	Bacteria	Gaiella	both
5.78	2	bASV_571	Bacteria	Kineosporia	rhizosphere
4.53	1.53	bASV_103	Bacteria	(Acetobacteraceae)	rhizosphere
4.15	1.46	fASV_106	Fungi	Microdochium	both
3.78	1.3	bASV_329	Bacteria	(Chitinophagaceae)	rhizosphere
-6.75	2.07	fASV_134	Fungi	Clonostachys	both
-6.87	2.38	bASV_594	Bacteria	Ramlibacter	both
-6.93	2.37	bASV_105	Bacteria	Rhodoplanes	leaf
-7.08	2.76	fASV_150	Fungi	(Fungi)	both
-7.44	2.98	fASV_126	Fungi	(Sordariomycetes)	leaf
-7.51	1.92	bASV_355	Bacteria	Geobacter	both
-8.27	2.76	fASV_498	Fungi	(GS11)	both
-9.17	3.11	fASV_112	Fungi	(Sordariales)	rhizosphere
-9.68	2.45	fASV_160	Fungi	Chaetomium	both
-13.21	2.19	fASV_114	Fungi	Humicola	rhizosphere
-21.72	3.13	fASV_21	Fungi	Rhizophydium	both
-23.11	3.14	fASV_68	Fungi	Curvularia	rhizosphere
-23.48	3.13	fASV_141	Fungi	Cercophora	leaf
-23.98	3.14	fASV_79	Fungi	Drechslera	rhizosphere
-24.14	2.79	fASV_256	Fungi	Pseudeurotium	rhizosphere

TABLE S3 | Top 20 genera by relative abundance in leaf and rhizosphere samples. Fungal groups that could not be identified at the genus level are indicated with parentheses.

Bacteria				Fungi			
Rhizosphere		Leaf		Rhizosphere		Leaf	
Ralstonia	0.375	Pantoea	0.5768	Entyloma	0.161	Entyloma	0.448
Burkholderia	0.137	Ralstonia	0.1101	Golubevia	0.133	Golubevia	0.265
Rhizobium	0.077	Herbaspirillum	0.0868	Tilletiopsis	0.1	Tilletiopsis	0.056
Dyella	0.07	Methylobacterium	0.0464	Vishniacozyma	0.067	(Chytridiomycota)	0.035
Mucilaginibacter	0.056	Sphingomonas	0.0344	Moesziomyces	0.053	unidentified	0.028
Chitinophaga	0.044	Bacillus	0.0314	Curvularia	0.049	(Chytridiomycetes)	0.026
Massilia	0.027	Methyloversatilis	0.0206	unidentified	0.04	Curvularia	0.016
Sphingobium	0.018	Curtobacterium	0.0134	Mycosphaerella	0.034	Spizellomyces	0.013
Sphingomonas	0.017	Massilia	0.0118	Boothiomyces	0.034	Boothiomyces	0.009
Bradyrhizobium	0.017	Staphylococcus	0.0085	(Pleosporaceae)	0.025	(Ustilaginaceae)	0.008
Mesorhizobium	0.011	Novosphingobium	0.0064	Pseudozyma	0.02	Pseudozyma	0.007
Acidovorax	0.01	Burkholderia	0.0058	(Ascomycota)	0.016	Vishniacozyma	0.006
Bacillus	0.01	Tumebacillus	0.0027	(Sordariomycetes)	0.015	Bipolaris	0.006
Duganella	0.008	Pseudomonas	0.0021	(Chytridiomycetes)	0.014	Cladosporium	0.005
Streptomyces	0.006	Rhizobium	0.002	Bipolaris	0.014	(Pleosporaceae)	0.005
Variovorax	0.005	Brevundimonas	0.0018	Ustilago	0.012	Moesziomyces	0.004
Arthrobacter	0.005	Corynebacterium	0.0017	Anthracocystis	0.011	(Dothideomycetes)	0.003
Rhodanobacter	0.005	Paenibacillus	0.0014	Dissoconium	0.009	Mycosphaerella	0.003
Herbaspirillum	0.005	Gardnerella	0.0014	(Sordariales)	0.008	(Chaetothyriales)	0.003
Niastella	0.004	Sphingobium	0.0014	Exophiala	0.008	(Leotiomycetes)	0.003

TABLE S4 | Host genotype influences alpha and beta diversity in maize leaf and rhizosphere microbiomes. ACE (log-transformed) and Shannon metrics were used to quantify community richness and evenness, respectively; Distance to centroid was used to quantify beta diversity (i.e., among-individual variation within genotypes). Bacterial **(a)** and fungal **(b)** communities were tested separately using univariate models and analysis of variance with Type III sums of squares and Satterthwaite's approximate denominator d.f. Likelihood ratio tests were used for significance testing of random-intercept effects. For rhizosphere fungal communities, one genotype (Oh43) was excluded from the analysis because no individuals survived in one field. *** $P < 0.001$; ** $P < 0.01$; * $P < 0.05$. All P-values were adjusted to correct for multiple comparisons using the Benjamini-Hochberg false discovery rate.

(a) Bacteria				
		ACE	**Shannon**	**Distance to centroid**
Leaf	Category	$F_{1,462} = 1.49$	$F_{1,14} = 0.39$	$F_{1,481} = 1.16$
	Field	$F_{1,44} = 0.91$	$F_{1,45} = 8.05$ *	$F_{1,50} = 5.51$ *
	Category x Field	$F_{1,460} = 1.1$	$F_{1,462} = 2.73$	$F_{1,479} = 3.69$
	Genotype	$\chi^2_1 = 0$	$\chi^2_1 = 1.03$	$\chi^2_1 = 0$
	Block	$\chi^2_1 = 5$	$\chi^2_1 = 1.65$	$\chi^2_1 = 0.08$
	Batch	$\chi^2_1 = 2.9$	$\chi^2_1 = 3.16$	$\chi^2_1 = 0.46$
	Sequencing depth	$F_{1,479} = 366.21$ ***	$F_{1,491} = 29.4$ ***	$F_{1,466} = 6.53$ *
		ACE	**Shannon**	**Distance to centroid**
Rhizosphere	Category	$F_{1,19} = 1.67$	$F_{1,20} = 0.16$***	$F_{1,15} = 10.6$ *
	Field	$F_{1,43} = 8.94$ **	$F_{1,43} = 0.13$	$F_{1,44} = 11.97$ **
	Category x Field	$F_{1,363} = 0$	$F_{1,364} = 1.85$	$F_{1,363} = 2.56$
	Collection date	$\chi^2_1 = 9.94$ **	$\chi^2_1 = 20.83$ ***	$\chi^2_1 = 4.9$ *
	Genotype	$\chi^2_1 = 21.77$ ***	$\chi^2_1 = 21.16$ ***	$\chi^2_1 = 9.86$ **
	Block	$\chi^2_1 = 27.31$ ***	$\chi^2_1 = 24.86$ ***	$\chi^2_1 = 28.07$ ***
	Batch	$\chi^2_1 = 2.78$	$\chi^2_1 = 3.16$	$\chi^2_1 = 8.79$ **
	Sequencing depth	$F_{1,350} = 1281.69$ ***	$F_{1,354} = 281.12$ ***	$F_{1,371} = 10.39$ **
(b) Fungi				
		ACE	**Shannon**	**Distance to centroid**
Leaf	Category	$F_{1,18} = 0.79$	$F_{1,14} = 0.58$	$F_{1,17} = 0$
	Field	$F_{1,50} = 26.31$ ***	$F_{1,44} = 30.14$ ***	$F_{1,50} = 57.32$ ***
	Category x Field	$F_{1,362} = 0$	$F_{17,441} = 0.37$	$F_{1,447} = 2.21$
	Genotype	$\chi^2_1 = 0.92$	$\chi^2_1 = 1.50$	$\chi^2_1 = 3.82$
	Block	$\chi^2_1 = 0.92$	$\chi^2_1 = 5.08$	$\chi^2_1 = 1.56$
	Batch	$\chi^2_1 = 30.45$ ***	$\chi^2_1 = 0.68$	$\chi^2_1 = 0.84$
	Sequencing depth	$F_{1,390} = 1255.92$ ***	$F_{1,353} = 23.34$ ***	$F_{1,362} = 16.66$ ***
		ACE	**Shannon**	**Distance to centroid**
Rhizosphere	Category	$F_{1,19} = 27.92$ ***	$F_{1,314} = 1.69$ ***	$F_{1,15} = 1.62$
	Field	$F_{1,36} = 18.21$ ***	$F_{1,39} = 48.22$ ***	$F_{1,46} = 0.03$
	Category x Field	$F_{1,309} = 3.05$	$F_{1,313} = 1.26$	$F_{1,317} = 0.43$
	Collection date	$\chi^2_1 = 2.33$	$\chi^2_1 = 1.38$	$\chi^2_1 = 1.48$
	Genotype	$\chi^2_1 = 0.02$ **	$\chi^2_1 = 0$	$\chi^2_1 = 2.06$
	Block	$\chi^2_1 = 7.83$ *	$\chi^2_1 = 6.44$ *	$\chi^2_1 = 0.99$
	Batch	$\chi^2_1 = 9.64$ **	$\chi^2_1 = 2.98$	$\chi^2_1 = 9.05$ **
	Sequencing depth	$F_{1,307} = 2085.31$ ***	$F_{1,245} = 74.52$ ****	$F_{1,316} = 24.54$ ***

TABLE S5 | ASVs showing significant midparent or "better parent" heterosis in at least one cross. This table can be downloaded as a separate tab-delimited (.txt) file. Each row summarizes one observation of midparent heterosis (MPH) or "better parent" heterosis (BPH) for one ASV in one hybrid. Column descriptions: Taxon = unique ID of the ASV; Maternal = genotype of maternal inbred line; Paternal = genotype of paternal inbred line; Hybrid = hybrid genotype; MatMean, PatMean, HybMean =

721 mean ASV abundance in the maternal, paternal, and hybrid genotype (residuals of variance-stabilized
722 counts after controlling for Field, Block, Batch, and sequencing depth); MatSE, PatSE, HybSE = standard
723 errors associated with the previously described means; Midparent = expected midparent value of ASV
724 abundance (average of MatMean and PatMean); BetterParent = defined as whichever of MatMean and
725 PatMean is closer to the HybMean; Type = whether heterosis was observed in leaf or rhizosphere;
726 MPH.t.stat, MPH.t.df, MPH.p, MPH.padj = test statistic, degrees of freedom, raw *P*-value, and FDR-
727 corrected *P*-value for T-test comparing HybMean to Midparent; BPH.t.stat, BPH.t.df, BPH.p, BPH.padj =
728 same statistics for T-test comparing HybMean to BetterParent; HetType = BPH if T-test provided
729 evidence for "better parent" heterosis, MPH if T-test supported midparent heterosis but not "better parent"
730 heterosis (ASVs with evidence for neither are not included in this table); Kingdom, Phylum, Class, Order,
731 Family, Genus, Sequence = taxonomic assignment and observed ITS1 or 16S-v4 sequence of the ASV;
732 Colonized = whether the ASV was present in the leaf dataset, rhizosphere dataset, or both.
733
734
735 **TABLE S6 | ASVs with strong loadings on axes of variation with high frequency of heterosis.** This
736 table can be downloaded as a separate tab-delimited (.txt) file.
737
738

TABLE S7 | Permutational MANOVA of fungal and bacterial community composition among genotypes within hybrid/inbred categories. *P*-values were generated from 999 permutations of Bray-Curtis dissimilarities among samples, which were calculated based on the matrix of variance-stabilized counts of amplicon sequence variants (ASVs). Permutations were constrained within Block and within Category.

		Bacteria			Fungi		
		R^2	pseudo-F test	P	R^2	pseudo-F test	P
Leaf	Sequencing depth	0.014	$F_{1,499} = 7.06$	0.001	0.027	$F_{1,478} = 14.73$	0.001
	Genotype	0.043	$F_{17,483} = 1.33$	0.001	0.036	$F_{17,462} = 1.15$	0.092
	Field	0.021	$F_{1,499} = 10.94$	0.527	0.075	$F_{1,478} = 40.15$	0.691
	Genotype x Field	0.034	$F_{17,483} = 1.03$	0.166	0.036	$F_{17,462} = 1.15$	0.011
		R^2	pseudo-F test	P	R^2	pseudo-F test	P
Rhizosphere	Sequencing depth	0.044	$F_{1,398} = 24.67$	0.001	0.038	$F_{1,329} = 19.41$	0.001
	Collection date	0.082	$F_{3,396} = 15.42$	0.001	0.074	$F_{3,327} = 12.67$	0.001
	Genotype	0.066	$F_{17,382} = 2.17$	0.001	0.063	$F_{17,313} = 1.92$	0.001
	Field	0.132	$F_{1,398} = 74.37$	0.001	0.226	$F_{1,329} = 116.40$	0.001

	Genotype x Field	0.033	$F_{17,382} = 1.08$	0.015	0.033	$F_{16,314} = 1.05$	0.240

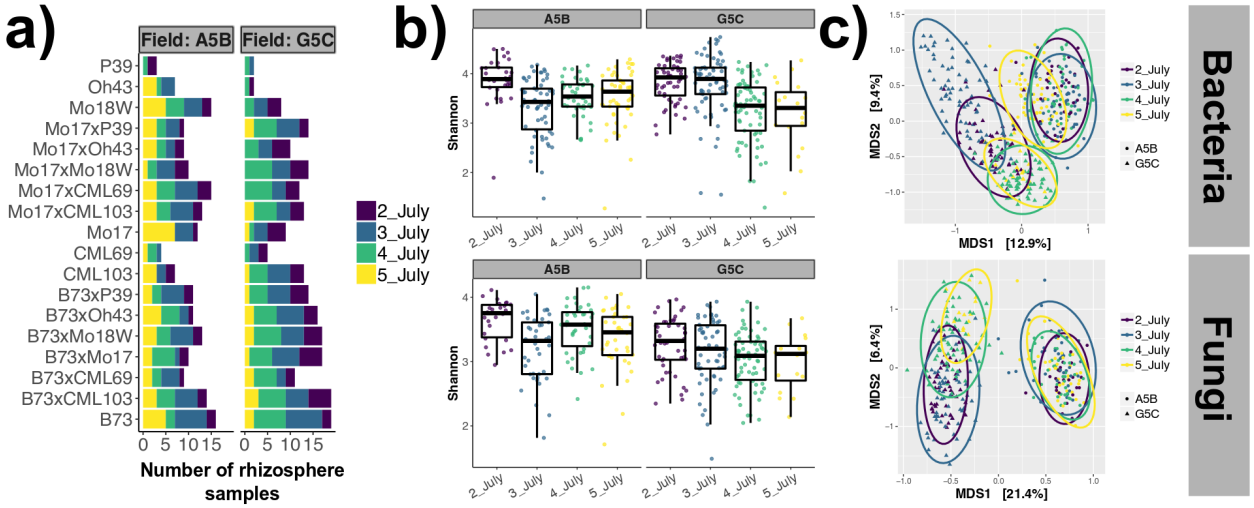

Figure S1 | The effect of collection date on rhizosphere microbiome diversity and composition. (a) The number of rhizosphere samples in the 16S dataset are shown for each host genotype in each field. Complete replicates were collected on each day so that collection date would not be confounded with either field or plant genotype; however, some genotypes with poor survival are not represented on all dates. **(b)** Shannon diversity varied slightly among collection dates for both bacteria (top) and fungi (bottom). **(c)** Principal coordinates analysis of Bray-Curtis dissimilarities shows that both bacterial and fungal communities shifted in community structure between July 3rd and July 4th, but only in one of the two fields (field G5C).

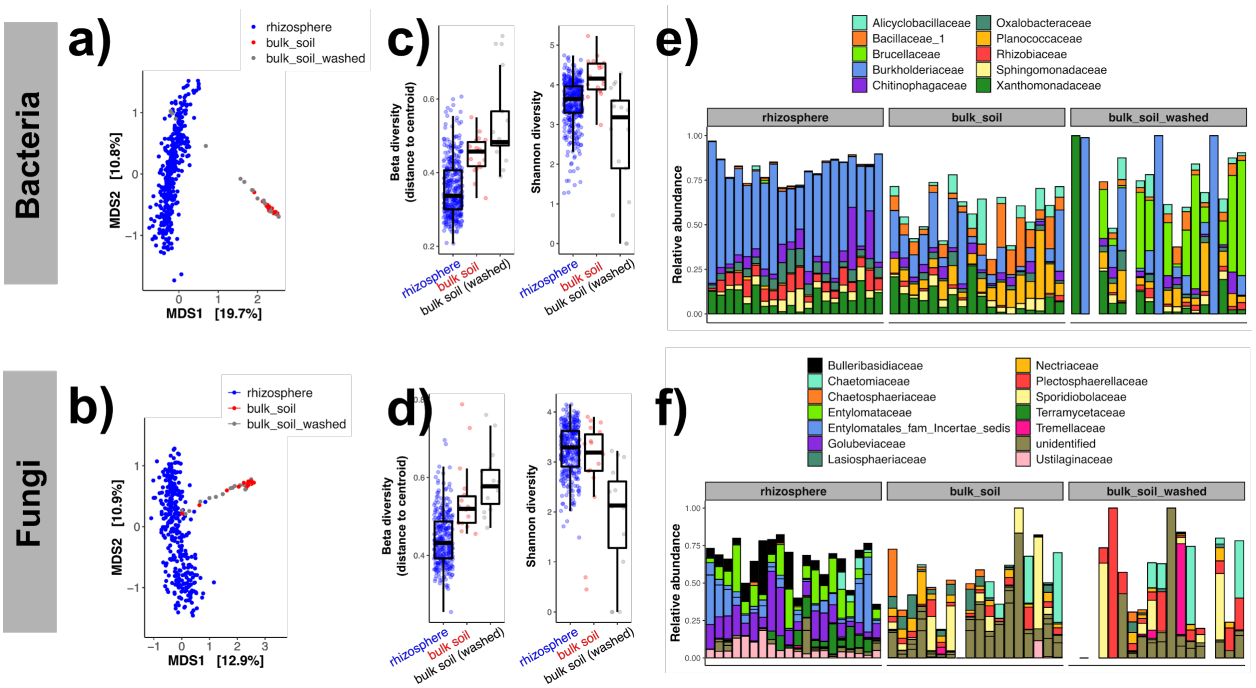

Figure S2 | Microbiome characteristics of rhizosphere, bulk soil, and "washed" bulk soil samples. Rhizosphere soil was collected from maize roots using a series of washes and centrifuge steps (see Methods). To assess the effects of this protocol on microbiome readouts, we divided each of 20 bulk soil samples into two aliquots and applied the same protocol to one aliquot prior to DNA extraction. **(a-b)** Multidimensional scaling reveals that bulk soil microbiomes differ substantially in composition from rhizosphere microbiomes, regardless of whether the washing protocol was applied. **(c-d)** For both bacterial and fungal microbiomes, the washing protocol increased beta diversity (left); therefore, the beta diversity values reported for rhizosphere samples in our study is likely an overestimate. The washing protocol decreased alpha diversity (right; measured using the Shannon diversity metric) of both bacterial and fungal communities in bulk soil; therefore, alpha diversity may have been underestimated for the rhizosphere samples in our study if this was due to exclusion or reduction of certain organisms by the protocol. Alternatively, the decrease in alpha diversity may reflect the removal of relic DNA that was artificially inflating diversity estimates, in which case the washing protocol may have increased data accuracy. **(e-f)** Microbiome composition at the family level is shown for randomly selected rhizosphere, bulk soil, and washed bulk soil samples. The 10 most abundant bacterial families and 14 most abundant fungal families are shown. The washing protocol caused notable increases in the relative abundance of Brucellaceae and Plectosphaerellaceae in bulk soil; however, neither of these groups was prominent in the rhizosphere samples.

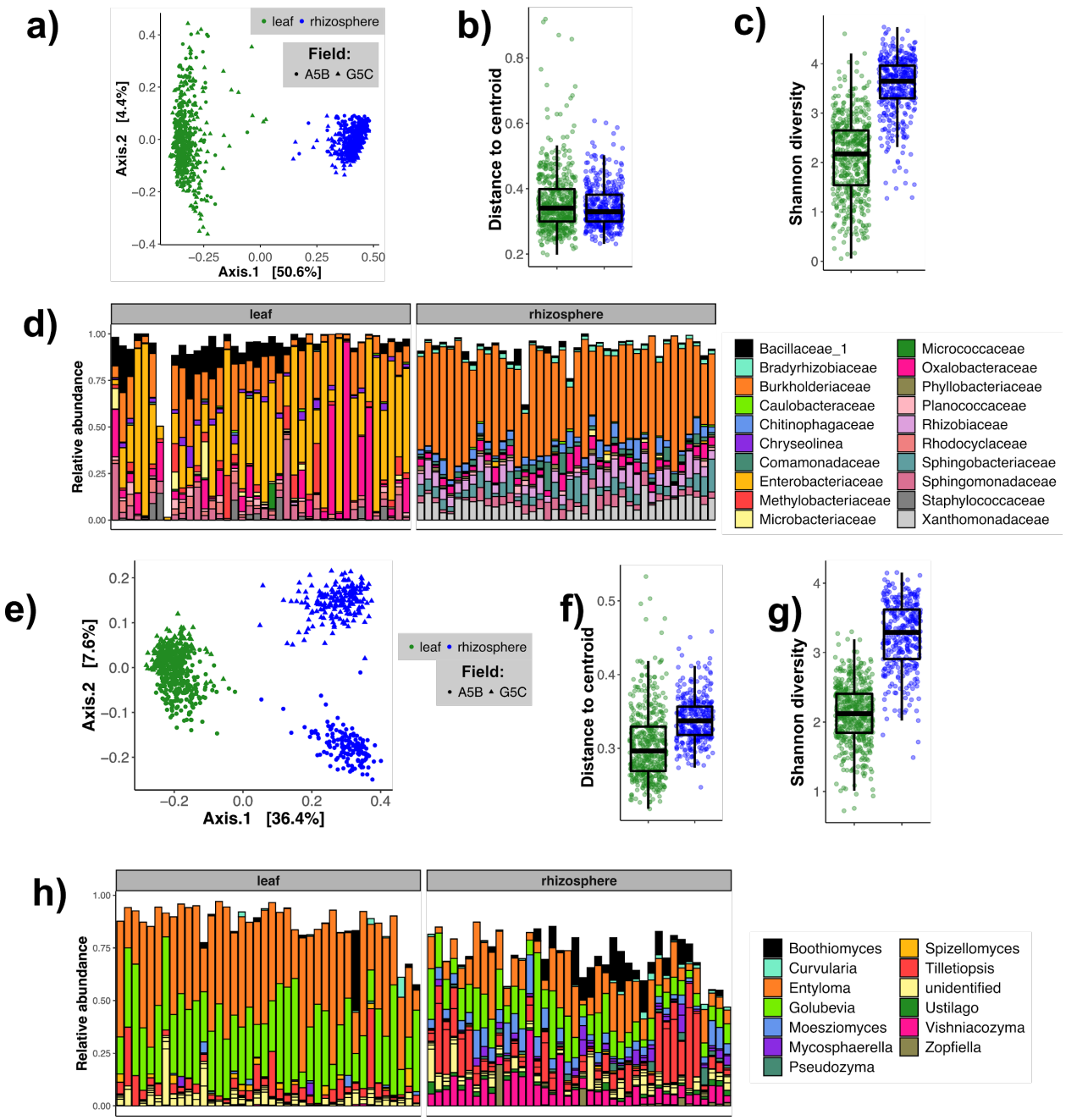

Figure S3 | Maize leaves and rhizosphere harbored distinct bacterial (top) and fungal (bottom) microbiomes. (a,e) Principal coordinates analysis of Bray-Curtis dissimilarities highlights the difference between leaf and rhizosphere microbial communities. **(b,f)** Beta diversity, measured as distance to centroid (based on Bray-Curtis dissimilarity), was higher in the rhizosphere for fungal communities only. The 75th and 25th percentiles are marked by the top and bottom of each box; the median is marked by the center line; and the length of each whisker is 1.5 times the interquartile range. **(c,g)** Alpha diversity was substantially higher for rhizosphere microbial communities than for leaf communities. Boxplot statistics are the same as for panels (c-d). **(d,h)** Leaf and rhizosphere communities were easily distinguished by bacterial and fungal community composition. Each column shows the taxonomic composition of one individual plant, randomly chosen from the dataset.

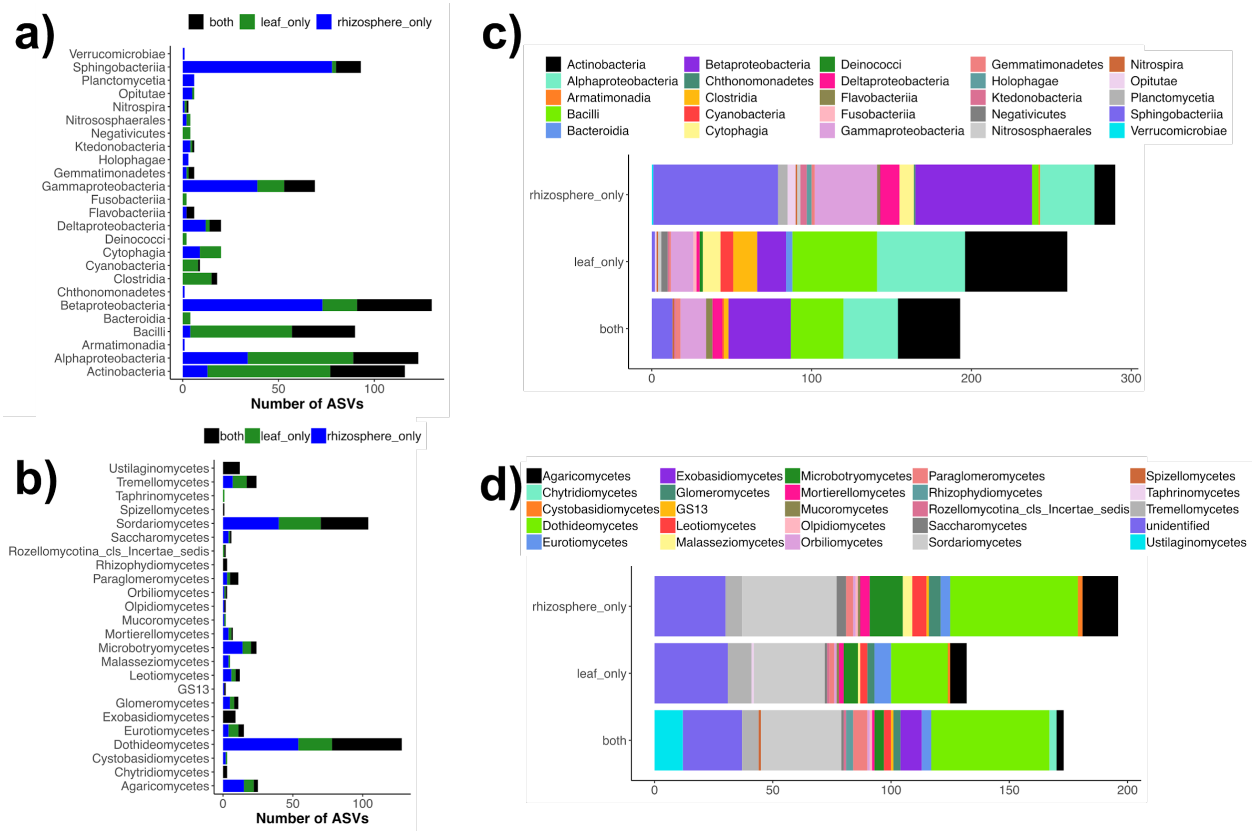

Figure S4 | A large minority of bacterial and fungal ASVs were observed in both leaves and rhizosphere. (a-b) For each bacterial and fungal class, the total number of ASVs is shown as well as the number of ASVs that were observed only in leaves, only in rhizosphere, or in both compartments. (c-d) The same data are shown to emphasize the taxonomic makeup of rhizosphere-specific, leaf-specific, and shared ASVs.

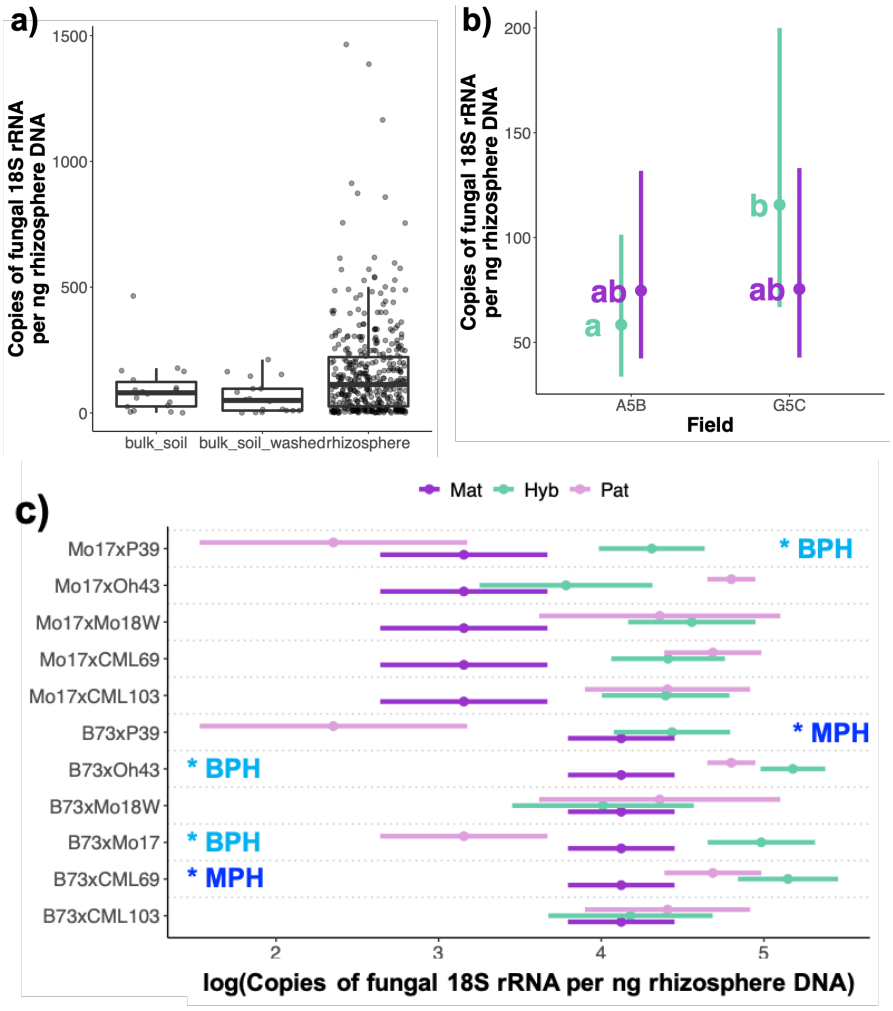

Figure S5 | Droplet digital PCR was used to quantify fungal load as the number of copies of fungal 18S rRNA per ng of DNA extracted from soil or rhizosphere samples. (a) Fungi made up a greater proportion of the rhizosphere microbiome than the bulk soil microbiome (ANOVA based on linear mixed-effects model of log-transformed fungal load, with Batch as a random-intercept term; $F_{2,425} = 6.02$; $P = 0.0026$). **(b)** For hybrid maize (green) but not inbred maize (purple), fungi made up a greater proportion of the rhizosphere microbiome in field G5C than in A5B (ANOVA, Category x Field $P < 0.05$; post-hoc Tukey's Honest Significant Differences are shown). However, on average there was no difference between hybrids and inbreds. **(c)** We detected heterosis of fungal load (log-transformed) in five hybrids. Mean values (+/- 1 s.e.m.) are shown for the maternal ("Mat") and paternal ("Pat") genotypes and the F1 hybrid ("Hyb") for each cross. *T*-tests were used to test for midparent and "better parent" heterosis as described in the Methods section of the main text. Statistical support (at $P < 0.05$) for midparent or "better parent" heterosis is noted with "*MPH" and "*BPH", respectively.

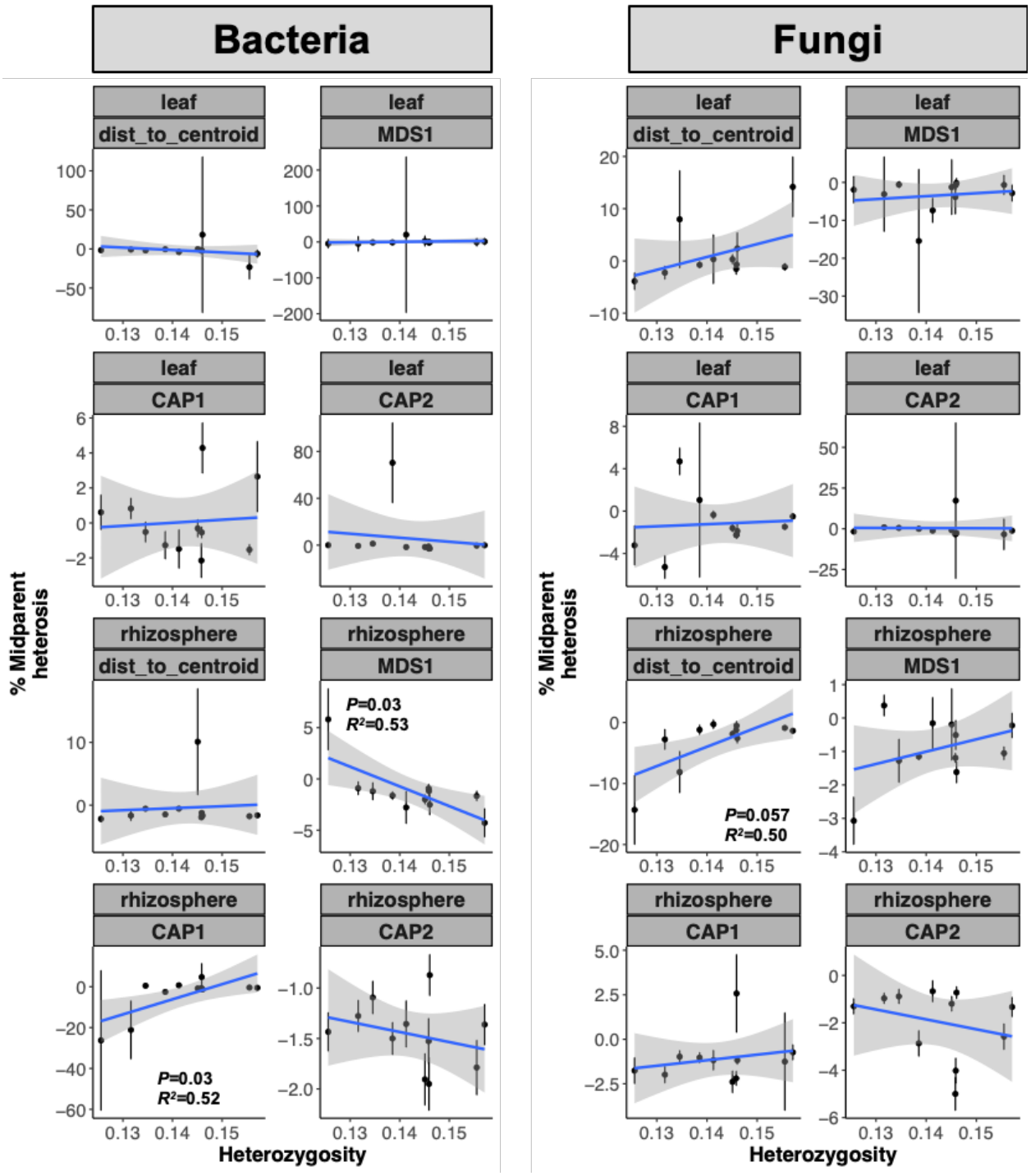

Figure S6 | Heterozygosity did not reliably predict heterosis of microbiome composition. For each hybrid, we used genome-wide heterozygosity to predict heterosis of microbiome properties (calculated as the percent change relative to the expected midparent value). Results of linear models are provided; unless otherwise shown, $P > 0.1$ after correction for false discovery rate.

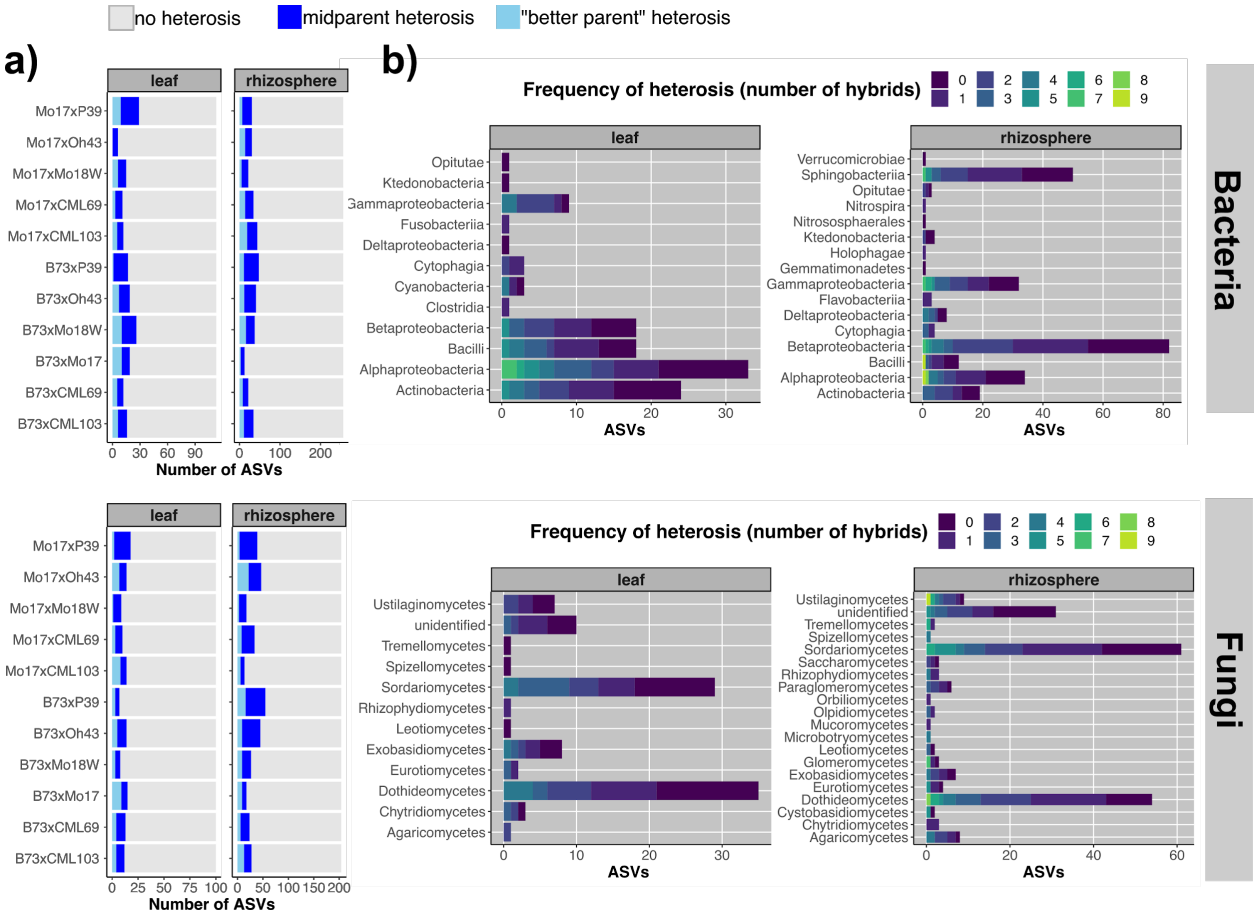

Figure S7 | The relative abundances of approximately 35-40% of all rhizosphere ASVs and 17-20% of all leaf ASVs were heterotic in at least one cross. (a) The majority of ASVs tested did not show any signal of heterosis in most crosses. ASV heterosis was more common in some hybrids than in others. **(b)** A diverse set of ASVs showed heterosis of relative abundance in at least one hybrid. The *x*-axis portrays the number of ASVs in each taxonomic class, colored according to the number of hybrids in which its abundance deviated from the midparent expectation (Figure 1). Bright colors represent ASVs that showed heterosis in many hybrids; dark colors represent ASVs that were rarely heterotic.

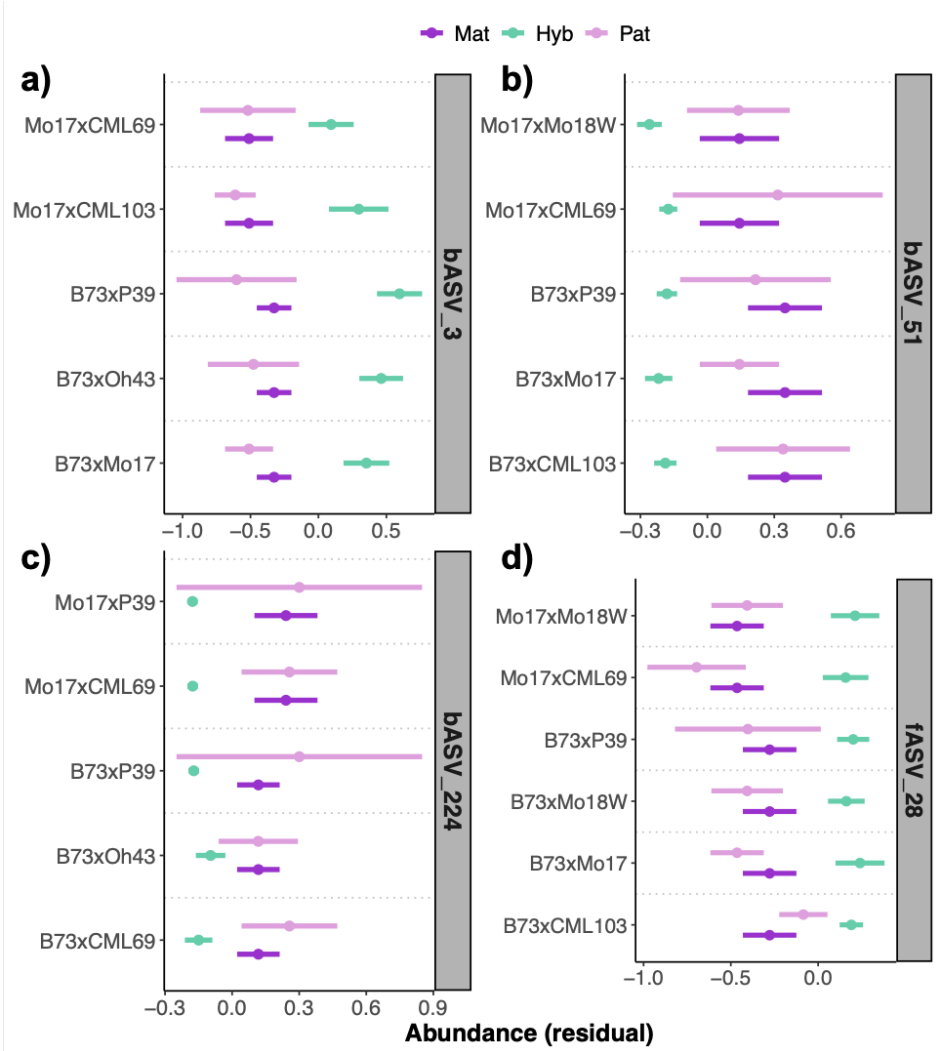

Figure S8 | The four taxa showing "better parent" heterosis most frequently. The mean abundance +/- 1 s.e.m. (residuals of variance-stabilized abundances, after controlling for Field, Block, Batch, and Sequencing depth) is plotted for each taxon in the maternal inbred parent ("Mat"), the paternal inbred parent ("Pat"), and the hybrid ("Hyb"). All contrasts between the hybrid and the inbred parents were statistically significant after correction for false discovery rate (*T*-test, FDR < 0.05). **(a)** "bASV_3" belonged to the genus *Pseudonocardia* and showed "better parent" heterosis in the rhizospheres of 5 hybrids. **(b)** "bASV_51" belonged to the genus *Acinetobacter* and showed "better parent" heterosis in the leaves of 5 hybrids. **(c)** "bASV_224" belonged to the genus *Sphingomonas* and showed "better parent" heterosis in the rhizospheres of 5 hybrids. **(d)** "fASV_28" belonged to *Moesziomyces aphidis* and showed "better parent" heterosis in the rhizospheres of 6 hybrids.

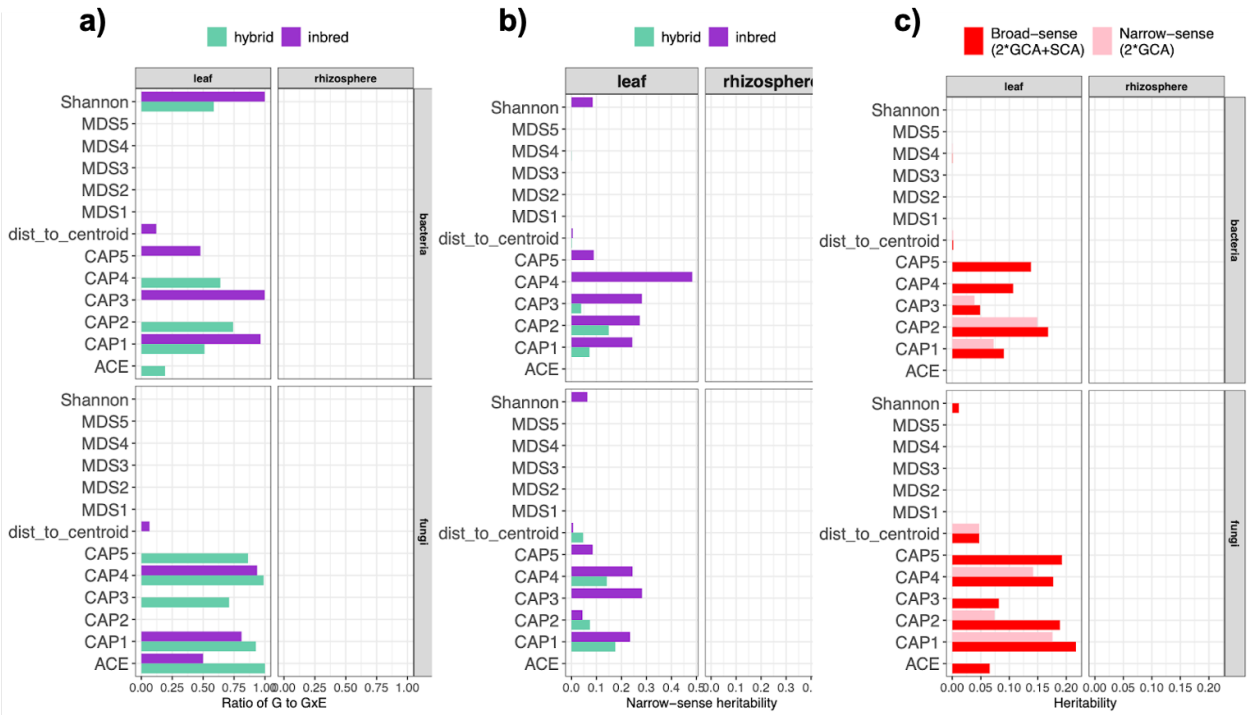

Figure S9 | Results of hybrid diallel analysis using linear mixed-effects models for inbreds and hybrids. (a) Variance components for Genotype and Genotype-Environment interactions (GxE) were calculated for each trait in hybrids and inbreds, separately. The ratio of G to GxE is plotted for each trait. Higher values indicate lower sensitivity to environmental variation. **(b)** Narrow-sense heritability (due to additive genetic effects) of each trait was calculated for inbreds and for hybrids. **(c)** For hybrids, narrow-sense heritability and broad-sense heritability (non-additive effects) are plotted for each trait. Substantially higher levels of broad-sense heritability indicate an influence of specific parental combinations, beyond the general combining ability (additive effects) of those parents.

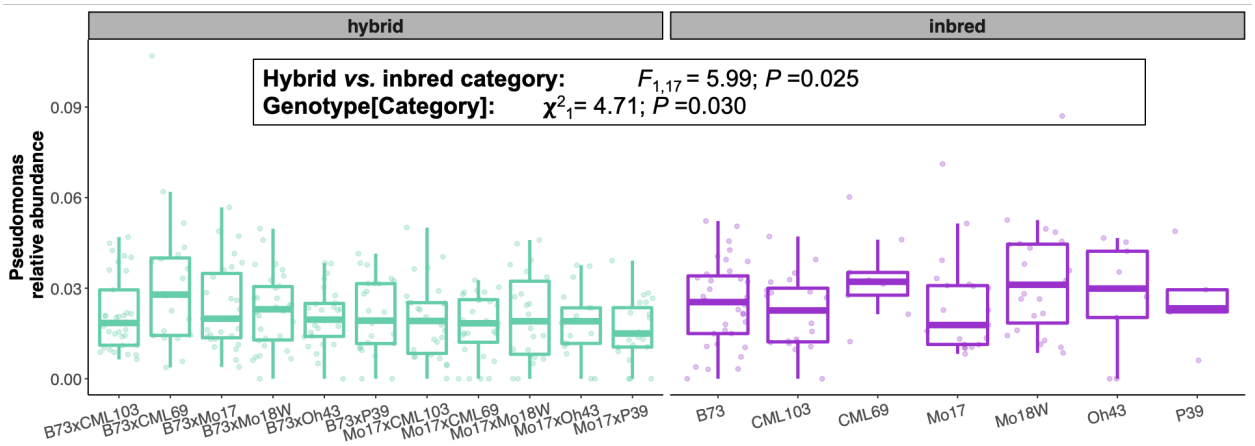

Figure S10 | Relative abundance of *Pseudomonas* spp. in the maize rhizosphere 7 weeks after planting. Relative abundances were modeled using hybrid/inbred Category, Field, and their interaction as fixed effect predictors, with Genotype, Block, and Batch as random-intercept terms.

858 **REFERENCES**

859 **Anderson E, Stebbins GL**. **1954**. HYBRIDIZATION AS AN EVOLUTIONARY STIMULUS.
860 *Evolution* **8**: 378–388.

861 **An G-H, -H. An G, Kobayashi S, Enoki H, Sonobe K, Muraki M, Karasawa T, Ezawa T**.
862 **2010**. How does arbuscular mycorrhizal colonization vary with host plant genotype? An example
863 based on maize (Zea mays) germplasms. *Plant and Soil* **327**: 441–453.

864 **Bates D, Mächler M, Bolker B, Walker S**. **2015**. Fitting Linear Mixed-Effects Models
865 Usinglme4. *Journal of Statistical Software* **67**.

866 **Beckers B, Op De Beeck M, Weyens N, Van Acker R, Van Montagu M, Boerjan W,**
867 **Vangronsveld J**. **2016**. Lignin engineering in field-grown poplar trees affects the endosphere
868 bacterial microbiome. *Proceedings of the National Academy of Sciences of the United States of*
869 *America* **113**: 2312–2317.

870 **Benjamini Y, Hochberg Y**. **1995**. Controlling the False Discovery Rate: A Practical and
871 Powerful Approach to Multiple Testing. *Journal of the Royal Statistical Society: Series B*
872 *(Methodological)* **57**: 289–300.

873 **Berg M, Koskella B**. **2018**. Nutrient- and Dose-Dependent Microbiome-Mediated Protection
874 against a Plant Pathogen. *Current biology: CB* **28**: 2487–2492.e3.

875 **Bevivino A, Dalmastri C, Tabacchioni S, Chiarini L**. **2000**. Efficacy of Burkholderia cepacia
876 MCI 7 in disease suppression and growth promotion of maize. *Biology and Fertility of Soils* **31**:
877 225–231.

878 **Birchler JA, Auger DL, Riddle NC**. **2003**. In search of the molecular basis of heterosis. *The*
879 *Plant cell* **15**: 2236–2239.

880 **Blum A**. **2013**. Heterosis, stress, and the environment: a possible road map towards the
881 general improvement of crop yield. *Journal of experimental botany* **64**: 4829–4837.

882 **Bodenhausen N, Bortfeld-Miller M, Ackermann M, Vorholt JA**. **2014**. A synthetic community
883 approach reveals plant genotypes affecting the phyllosphere microbiota. *PLoS genetics* **10**:
884 e1004283.

885 **Bodenhausen N, Horton MW, Bergelson J**. **2013**. Bacterial Communities Associated with the
886 Leaves and the Roots of Arabidopsis thaliana. *PLoS ONE* **8**: e56329.

887 **Bordenstein SR, Theis KR**. **2015**. Host Biology in Light of the Microbiome: Ten Principles of
888 Holobionts and Hologenomes. *PLOS Biology* **13**: e1002226.

889 **Bressan M, Roncato M-A, Bellvert F, Comte G, el Zahar Haichar F, Achouak W, Berge O**.
890 **2009**. Exogenous glucosinolate produced by Arabidopsis thaliana has an impact on microbes in
891 the rhizosphere and plant roots. *The ISME Journal* **3**: 1243–1257.

892 **Brucker RM, Bordenstein SR**. **2013**. The hologenomic basis of speciation: gut bacteria cause
893 hybrid lethality in the genus Nasonia. *Science* **341**: 667–669.

894 **Buckler ES, Holland JB, Bradbury PJ, Acharya CB, Brown PJ, Browne C, Ersoz E, Flint-**
895 **Garcia S, Garcia A, Glaubitz JC, *et al.* 2009**. The genetic architecture of maize flowering time.

Science **325**: 714–718.

Busby PE, Peay KG, Newcombe G. **2016**. Common foliar fungi of Populus trichocarpa modify Melampsora rust disease severity. *The New phytologist* **209**: 1681–1692.

Busby PE, Soman C, Wagner MR, Friesen ML, Kremer J, Bennett A, Morsy M, Eisen JA, Leach JE, Dangl JL. **2017**. Research priorities for harnessing plant microbiomes in sustainable agriculture. *PLoS biology* **15**: e2001793.

Callahan BJ, McMurdie PJ, Rosen MJ, Han AW, Johnson AJA, Holmes SP. **2016**. DADA2: High-resolution sample inference from Illumina amplicon data. *Nature methods* **13**: 581–583.

Chaney L, Baucom RS. **2020**. The soil microbial community alters patterns of selection on flowering time and fitness-related traits in Ipomoea purpurea. *American Journal of Botany* **107**: 186–194.

Chia J-M, Song C, Bradbury PJ, Costich D, de Leon N, Doebley J, Elshire RJ, Gaut B, Geller L, Glaubitz JC, *et al.* 2012. Maize HapMap2 identifies extant variation from a genome in flux. *Nature genetics* **44**: 803–807.

Coleman-Derr D, Desgarennes D, Fonseca-Garcia C, Gross S, Clingenpeel S, Woyke T, North G, Visel A, Partida-Martinez LP, Tringe SG. **2016**. Plant compartment and biogeography affect microbiome composition in cultivated and native Agave species. *The New phytologist* **209**: 798–811.

Cole JR, Wang Q, Fish JA, Chai B, McGarrell DM, Sun Y, Brown CT, Porras-Alfaro A, Kuske CR, Tiedje JM. **2014**. Ribosomal Database Project: data and tools for high throughput rRNA analysis. *Nucleic acids research* **42**: D633–42.

Cregger MA, Veach AM, Yang ZK, Crouch MJ, Vilgalys R, Tuskan GA, Schadt CW. **2018**. The Populus holobiont: dissecting the effects of plant niches and genotype on the microbiome. *Microbiome* **6**: 31.

De León C. **1978**. *Maize Diseases: A Guide for Field Identification*.

Edwards J, Johnson C, Santos-Medellín C, Lurie E, Podishetty NK, Bhatnagar S, Eisen JA, Sundaresan V. **2015**. Structure, variation, and assembly of the root-associated microbiomes of rice. *Proceedings of the National Academy of Sciences of the United States of America* **112**: E911–20.

Flint-Garcia SA, Buckler ES, Tiffin P, Ersoz E, Springer NM. **2009**. Heterosis is prevalent for multiple traits in diverse maize germplasm. *PloS one* **4**: e7433.

Friesen ML, Porter SS, Stark SC, von Wettberg EJ, Sachs JL, Martinez-Romero E. **2011**. Microbially Mediated Plant Functional Traits. *Annual Review of Ecology, Evolution, and Systematics* **42**: 23–46.

Fusseder A. **1987**. The longevity and activity of the primary root of maize. *Plant and Soil* **101**: 257–265.

Griffing B, Zsiros E. **1971**. Heterosis associated with genotype-environment interactions. *Genetics* **68**: 443–455.

Guo T, Yu X, Li X, Zhang H, Zhu C, Flint-Garcia S, McMullen MD, Holland JB, Szalma SJ, Wisser RJ, *et al.* 2019. Optimal Designs for Genomic Selection in Hybrid Crops. *Molecular Plant* **12**: 390–401.

Horton MW, Bodenhausen N, Beilsmith K, Meng D, Muegge BD, Subramanian S, Vetter MM, Vilhjálmsson BJ, Nordborg M, Gordon JI, *et al.* 2014. Genome-wide association study of Arabidopsis thaliana leaf microbial community. *Nature communications* **5**: 5320.

Hubbard CJ, Li B, McMinn R, Brock MT, Maignien L, Ewers BE, Kliebenstein D, Weinig C. **2019**. The effect of rhizosphere microbes outweighs host plant genetics in reducing insect herbivory. *Molecular ecology* **28**: 1801–1811.

Hughes JB, Hellmann JJ, Ricketts TH, Bohannan BJ. **2001**. Counting the uncountable: statistical approaches to estimating microbial diversity. *Applied and environmental microbiology* **67**: 4399–4406.

Isik F, Holland J, Maltecca C. **2017**. Genetic Data Analysis for Plant and Animal Breeding.

Jiao Y, Peluso P, Shi J, Liang T, Stitzer MC, Wang B, Campbell MS, Stein JC, Wei X, Chin C-S, *et al.* 2017. Improved maize reference genome with single-molecule technologies. *Nature* **546**: 524–527.

Korsman J, Meisel B, Kloppers FJ, Crampton BG, Berger DK. **2012**. Quantitative phenotyping of grey leaf spot disease in maize using real-time PCR. *European Journal of Plant Pathology* **133**: 461–471.

Kuznetsova A, Brockhoff PB, Christensen RHB. **2017**. lmerTest Package: Tests in Linear Mixed Effects Models. *Journal of Statistical Software* **82**.

Lau JA, Lennon JT. **2012**. Rapid responses of soil microorganisms improve plant fitness in novel environments. *Proceedings of the National Academy of Sciences of the United States of America* **109**: 14058–14062.

Lebeis SL, Paredes SH, Lundberg DS, Breakfield N, Gehring J, McDonald M, Malfatti S, del Rio TG, Jones CD, Tringe SG, *et al.* 2015. Salicylic acid modulates colonization of the root microbiome by specific bacterial taxa. *Science* **349**: 860–864.

Lemanceau P, Blouin M, Muller D, Moënne-Loccoz Y. **2017**. Let the Core Microbiota Be Functional. *Trends in Plant Science* **22**: 583–595.

Lewis D. **1954**. Gene-environment interaction: A relationship between dominance, heterosis, phenotypic stability and variability. *Heredity* **8**: 333–356.

Li Z, Coffey L, Garfin J, Miller ND, White MR, Spalding EP, de Leon N, Kaeppler SM, Schnable PS, Springer NM, *et al.* 2018. Genotype-by-environment interactions affecting heterosis in maize. *PloS one* **13**: e0191321.

Liu CM, Kachur S, Dwan MG, Abraham AG, Aziz M, Hsueh P-R, Huang Y-T, Busch JD, Lamit LJ, Gehring CA, *et al.* 2012. FungiQuant: A broad-coverage fungal quantitative real-time PCR assay. *BMC Microbiology* **12**: 255.

Love MI, Huber W, Anders S. **2014**. Moderated estimation of fold change and dispersion for RNA-seq data with DESeq2. *Genome biology* **15**: 550.

Lundberg DS, Lebeis SL, Paredes SH, Yourstone S, Gehring J, Malfatti S, Tremblay J, Engelbrektson A, Kunin V, Del Rio TG, *et al.* 2012. Defining the core Arabidopsis thaliana root microbiome. *Nature* **488**: 86–90.

Lundberg DS, Yourstone S, Mieczkowski P, Jones CD, Dangl JL. **2013**. Practical innovations for high-throughput amplicon sequencing. *Nature methods* **10**: 999–1002.

Maignien L, DeForce EA, Chafee ME, Eren AM, Simmons SL. **2014**. Ecological succession and stochastic variation in the assembly of Arabidopsis thaliana phyllosphere communities. *mBio* **5**: e00682–13.

Martin M. **2011**. Cutadapt removes adapter sequences from high-throughput sequencing reads. *EMBnet.journal* **17**: 10.

McMurdie PJ, Holmes S. **2013**. phyloseq: an R package for reproducible interactive analysis and graphics of microbiome census data. *PloS one* **8**: e61217.

McMurdie PJ, Holmes S. **2014**. Waste Not, Want Not: Why Rarefying Microbiome Data Is Inadmissible. *PLoS Computational Biology* **10**: e1003531.

Mitter B, Petric A, Chain PSG, Trognitz F, Nowak J, Compant S, Sessitsch A. **2013**. Genome Analysis, Ecology, and Plant Growth Promotion of the Endophyte Burkholderia phytofirmans Strain PsJN. *Molecular Microbial Ecology of the Rhizosphere*: 865–874.

Möhring J, Melchinger AE, Piepho HP. **2011**. REML-Based Diallel Analysis. *Crop Science* **51**: 470.

Nilsson RH, Larsson K-H, Taylor AFS, Bengtsson-Palme J, Jeppesen TS, Schigel D, Kennedy P, Picard K, Glöckner FO, Tedersoo L, *et al.* 2019. The UNITE database for molecular identification of fungi: handling dark taxa and parallel taxonomic classifications. *Nucleic acids research* **47**: D259–D264.

O'Brien AM, Sawers RJH, Strauss SY, Ross-Ibarra J. Adaptive phenotypic divergence in an annual grass differs across biotic contexts.

Oksanen JF, Blanchet G, Friendly M, Kindt R, Legendre P, McGlinn D, Minchin PR, O'Hara RB, Simpson GL, Solymos P, *et al.* 2019. *vegan: Community Ecology Package*.

Panke-Buisse K, Lee S, Kao-Kniffin J. **2017**. Cultivated Sub-Populations of Soil Microbiomes Retain Early Flowering Plant Trait. *Microbial ecology* **73**: 394–403.

Panke-Buisse K, Poole AC, Goodrich JK, Ley RE, Kao-Kniffin J. **2015**. Selection on soil microbiomes reveals reproducible impacts on plant function. *The ISME journal* **9**: 980–989.

Peiffer JA, Ley RE. **2013**. Exploring the maize rhizosphere microbiome in the field: A glimpse into a highly complex system. *Communicative & integrative biology* **6**: e25177.

Peiffer JA, Spor A, Koren O, Jin Z, Tringe SG, Dangl JL, Buckler ES, Ley RE. **2013**. Diversity and heritability of the maize rhizosphere microbiome under field conditions. *Proceedings of the National Academy of Sciences of the United States of America* **110**: 6548–6553.

Perin L, Martínez-Aguilar L, Castro-González R, Estrada-de Los Santos P, Cabellos-

1011 **Avelar T, Guedes HV, Reis VM, Caballero-Mellado J**. **2006**. Diazotrophic burkholderia
1012 species associated with field-grown maize and sugarcane. *Applied and environmental*
1013 *microbiology* **72**: 3103–3110.

1014 **Picard C, Baruffa E, Bosco M**. **2008**. Enrichment and diversity of plant-probiotic
1015 microorganisms in the rhizosphere of hybrid maize during four growth cycles. *Soil Biology and*
1016 *Biochemistry* **40**: 106–115.

1017 **Picard C, Bosco M**. **2005**. Maize heterosis affects the structure and dynamics of indigenous
1018 rhizospheric auxins-producing Pseudomonas populations. *FEMS Microbiology Ecology* **53**:
1019 349–357.

1020 **Picard C, Bosco M**. **2006**. Heterozygosis drives maize hybrids to select elite 2,4-
1021 diacethylphloroglucinol-producing Pseudomonas strains among resident soil populations. *FEMS*
1022 *microbiology ecology* **58**: 193–204.

1023 **Picard C, Frascaroli E, Bosco M**. **2004**. Frequency and biodiversity of 2,4-
1024 diacetylphloroglucinol-producing rhizobacteria are differentially affected by the genotype of two
1025 maize inbred lines and their hybrid. *FEMS Microbiology Ecology* **49**: 207–215.

1026 **Ponsford JCB, Hubbard CJ, Harrison JG, Maignien L, Alex Buerkle C, Weinig C**. Whole-
1027 genome duplication and host genotype affect rhizosphere microbial communities in Arabidopsis
1028 thaliana.

1029 **Prévost D, Gauvin-Trudel C, Juge C**. **2012**. Diversity of Bradyrhizobium populations
1030 associated to soybean–maize rotations in Québec, Eastern Canada, and their potential to
1031 improve growth of both plant species. *Applied Soil Ecology* **59**: 29–38.

1032 **Ritpitakphong U, Falquet L, Vimoltust A, Berger A, Métraux J-P, L'Haridon F**. **2016**. The
1033 microbiome of the leaf surface of Arabidopsis protects against a fungal pathogen. *The New*
1034 *phytologist* **210**: 1033–1043.

1035 **Robertson LA, Kleinschmidt CE, White DG, Payne GA, Maragos CM, Holland JB**. **2006**.
1036 Heritabilities and Correlations of Fusarium Ear Rot Resistance and Fumonisin Contamination
1037 Resistance in Two Maize Populations. *Crop Science* **46**: 353–361.

1038 **Santhanam R, Luu VT, Weinhold A, Goldberg J, Oh Y, Baldwin IT**. **2015**. Native root-
1039 associated bacteria rescue a plant from a sudden-wilt disease that emerged during continuous
1040 cropping. *Proceedings of the National Academy of Sciences of the United States of America*
1041 **112**: E5013–20.

1042 **Schnable PS, Springer NM**. **2013**. Progress toward understanding heterosis in crop plants.
1043 *Annual review of plant biology* **64**: 71–88.

1044 **Smercina DN, Evans SE, Friesen ML, Tiemann LK**. **2019**. To Fix or Not To Fix: Controls on
1045 Free-Living Nitrogen Fixation in the Rhizosphere. *Applied and Environmental Microbiology* **85**.

1046 **Soltis PS, Soltis DE**. **2009**. The role of hybridization in plant speciation. *Annual review of plant*
1047 *biology* **60**: 561–588.

1048 **Sun S, Zhou Y, Chen J, Shi J, Zhao H, Zhao H, Song W, Zhang M, Cui Y, Dong X, *et al.***
1049 **2018**. Extensive intraspecific gene order and gene structural variations between Mo17 and other

1050 maize genomes. *Nature genetics* **50**: 1289–1295.

1051 **Urquhart EJ**. **1994**. Growth and Biological Control Activity ofTilletiopsisSpecies Against
1052 Powdery Mildew (Sphaerotheca fuliginea) on Greenhouse Cucumber. *Phytopathology* **84**: 341.

1053 **Urquhart EJ, Punja ZK**. **2002**. Hydrolytic enzymes and antifungal compounds produced by
1054 Tilletiopsis species, phyllosphere yeasts that are antagonists of powdery mildew fungi.
1055 *Canadian journal of microbiology* **48**: 219–229.

1056 **Van Esbroeck GA, Ruiz Corral JA, Sanchez Gonzalez JJ, Holland JB**. **2008**. A
1057 COMPARISON OF LEAF APPEARANCE RATES AMONG TEOSINTE,MAIZE LANDRACES
1058 AND MODERN MAIZE. *Maydica* **53**: 117–123.

1059 **Vorholt JA, Vogel C, Carlström CI, Müller DB**. **2017**. Establishing Causality: Opportunities of
1060 Synthetic Communities for Plant Microbiome Research. *Cell Host & Microbe* **22**: 142–155.

1061 **Wagner MR, Busby PE, Balint-Kurti P**. **2020**. Analysis of leaf microbiome composition of near-
1062 isogenic maize lines differing in broad-spectrum disease resistance. *New Phytologist* **225**:
1063 2152–2165.

1064 **Wagner MR, Lundberg DS, Coleman-Derr D, Tringe SG, Dangl JL, Mitchell-Olds T**. **2014**.
1065 Natural soil microbes alter flowering phenology and the intensity of selection on flowering time in
1066 a wild Arabidopsis relative. *Ecology letters* **17**: 717–726.

1067 **Wagner MR, Lundberg DS, Del Rio TG, Tringe SG, Dangl JL, Mitchell-Olds T**. **2016**. Host
1068 genotype and age shape the leaf and root microbiomes of a wild perennial plant. *Nature*
1069 *communications* **7**: 12151.

1070 **Wallace JG, Kremling KA, Kovar LL, Buckler ES**. **2018a**. Quantitative Genetics of the Maize
1071 Leaf Microbiome. *Phytobiomes Journal* **2**: 208–224.

1072 **Wallace J, Laforest-Lapointe I, Kembel SW**. **2018b**. Variation in the leaf and root microbiome
1073 of sugar maple (Acer saccharum) at an elevational range limit. *PeerJ* **6**: e5293.

1074 **Walters WA, Jin Z, Youngblut N, Wallace JG, Sutter J, Zhang W, González-Peña A, Peiffer**
1075 **J, Koren O, Shi Q, *et al.* 2018**. Large-scale replicated field study of maize rhizosphere identifies
1076 heritable microbes. *Proceedings of the National Academy of Sciences of the United States of*
1077 *America* **115**: 7368–7373.

1078 **Wang Q, Garrity GM, Tiedje JM, Cole JR**. **2007**. Naive Bayesian classifier for rapid
1079 assignment of rRNA sequences into the new bacterial taxonomy. *Applied and environmental*
1080 *microbiology* **73**: 5261–5267.

1081 **Wang J, Kalyan S, Steck N, Turner LM, Harr B, Künzel S, Vallier M, Häsler R, Franke A,**
1082 **Oberg H-H, *et al.* 2015**. Analysis of intestinal microbiota in hybrid house mice reveals
1083 evolutionary divergence in a vertebrate hologenome. *Nature Communications* **6**.

1084 **Wickham H**. **2017**. *tidyverse: Easily Install and Load the 'Tidyverse'*.

1085 **Yu J, Holland JB, McMullen MD, Buckler ES**. **2008**. Genetic design and statistical power of
1086 nested association mapping in maize. *Genetics* **178**: 539–551.

1087 **Zanewich KP, Pearce DW, Rood SB**. **2018**. Heterosis in poplar involves phenotypic stability:

cottonwood hybrids outperform their parental species at suboptimal temperatures. *Tree physiology* **38**: 789–800.